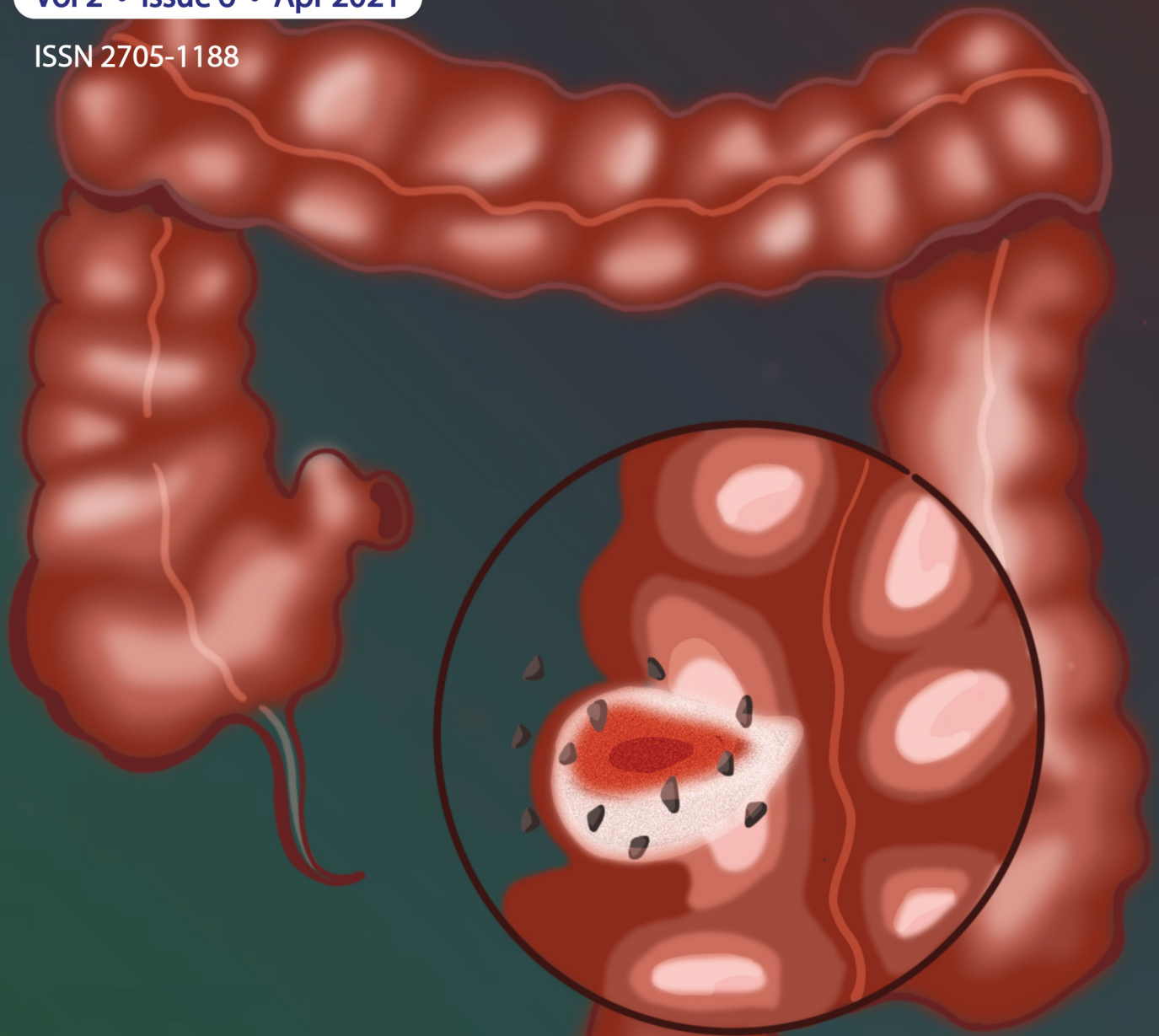


STEMedicine

Vol 2 • Issue 6 • Apr 2021

ISSN 2705-1188



MicroRNA-4284 inhibits colon cancer
epithelial-mesenchymal transition
by down-regulating Perilipin 5

STEMedicine

stemedicine.org

Microtubule dynamics in cytoskeleton, neurodegenerative and psychiatric disease

Simone MORTAL*

Neuroscience Area, International School for Advanced Studies (SISSA), 34136 Trieste, Italy

*Correspondence: smortal@sissa.it

<https://doi.org/10.37175/stemedicine.v2i6.81>

ABSTRACT

Microtubules (MTs) are fundamental polymers composed by α and β tubulin, they provide integrity to neuronal cell and are necessities in intracellular trafficking and organization. The extension and retraction of MTs occur with the addition or removal of α and β tubulin subunits and the binding with microtubule associated proteins (MAPs) that selectively target specific tubulin regions, manipulating the MT dynamics and function. Altered MT homeostasis can compromise the function of MTs in the structural integrity and axonal transport inside the neuron. Here I review the evidence of MT anomalies in several neurodegenerative diseases, including Alzheimer's disease, Parkinson disease, amyotrophic lateral sclerosis and traumatic brain injury and psychiatric disorders, such as depression, schizophrenia, and bipolar disorder. The focus of this review is to point out which can be the impact of MT issues in the major neurodegenerative diseases and discuss which MT abnormalities can lead to psychiatric illnesses.

Keywords: Microtubules · MAPs · Alzheimer's disease · Amyotrophic lateral sclerosis · Schizophrenia · Psychiatric disorders · Neurodegenerative diseases

Introduction

During the neuronal development stages, aside from the actin cytoskeleton, the assembly, organization and remodelling of the microtubule (MT) cytoskeleton is essential (1–3). MTs compose the rails for intracellular transport, they can act as signalling devices, generate cellular forces and mediate vesicular release (4–7).

The MT cytoskeleton is fundamental in neuronal development, this is highlighted by the wide range of nervous system abnormalities and several human neurodevelopmental disorders linked to altered MT-mediated processes. In addition, there are several developmental problems that can be linked to mutations in MT-related genes that encode for microtubule-associated proteins (MAPs), MT motor associated regulators or MT severing proteins (8,9).

In this review I examine how MTs are built, and which are the major proteins that interact with them. Then I analyse some of the most important neurodegenerative disorders exploring the interaction that connects disease with MT cytoskeleton. In the last part I discuss how anomalies in the MTs, or related proteins, can lead to psychiatric disease.

Microtubule organization

The MT structure is built from heterodimers of α and β tubulin, that are bound in a head to tail relation to form polarized structures; these associate laterally to form a hollow tube, with a diameter of 25 nm (5). MTs are very dynamic structures, that continuously switch between elongation and disassembly, in a process called dynamic instability; this procedure allows individual MT to explore cellular regions and to retract if it does not find the proper environment (10).

MT function and dynamics are regulated by the properties of tubulin; the free tubulin binds GTP, which is hydrolysed after being incorporated into the MT structure. The growth of the MT is promoted by the GTP cap, in

Received: Feb 8, 2021; Accepted: Mar 22, 2021.

© The Author(s). 2020 This is an **Open Access** article distributed under the terms of the Creative Commons License (<http://creativecommons.org/licenses/by/4.0/>) which permits unrestricted use, distribution, and reproduction in any medium or format, provided the original work is properly cited.

fact, GDP-tubulin tends to destabilize the MT architecture, consequently stable growth is believed to depend on the presence of a GTP-tubulin cap at the MT plus end (11). In this model, the loss of the cap will result in a collapse of the structure, called catastrophe (12).

At the end of the MT there is a minus end and a plus end, these ends can grow and depolymerize, but these two dynamics are completely different. Minus ends are stabilized by minus end tracking proteins (-TIPs), they grow more slowly and undergo catastrophe less rarely, not a lot is known about them, in fact they start to emerge recently (13). The plus end, terminate with β -tubulin, grows with polymerization of the subunits, undergoes catastrophe more frequently and is a crucial site for regulating MT dynamics (14).

Plus end tracking proteins (+TIPs) concentrate at the ends of growing MTs and control different aspects of its progress, like recruiting tubulin dimers and increasing the rate of tubulin addition to growing tips (15). Nevertheless, the polymerization of microtubule based structures not only depends on +TIPs, but also requires many other factors, like MAPs, motor proteins and tubulin isoforms (5).

Concentrating on the different ways of action, five groups of proteins can be assumed from the microtubule related proteins. Firstly, proteins that bind to the MT ends and can regulate their dynamics, this group contains the +TIPs and minus end targeting proteins (-TIPs) (5,14). Then, the group of proteins that binds to the MT lattice and can stabilize or crosslink MTs (16,17). The third group includes proteins that modulate the MT abundance, enzymes that sever MTs and regulators of the nucleation (18,19). The fourth group contains the kinesin and dynein families that generate forces and move directionally along MTs (20). The last group comprises tubulin folding cofactors and tubulin modifying enzymes that can generate distinct MT subtypes through post translational modifications (21) (**Figure 1**).

The Neuronal MT Cytoskeleton

The MTs of neurons are involved in the morphological changes during the different phases during their development, in the intracellular transport and during synapse growth.

Neurons need to have an active and efficient transport mechanism, to properly distribute many cellular components and establish signalling pathways. The motor protein families that play this role are Kinesins and dyneins, they travel along the neuronal MTs carrying many types of neuronal cargo: neurotransmitter receptors, synaptic vesicles, cell adhesion molecules, organelles, cell signalling molecules and mRNAs. In addition, cargo adaptor proteins, regulatory molecules and MT cytoskeleton have an important role in the delivering of different cargos in the correct location (20).

MTs are fundamental in the morphological transitions that occur during neuronal development: *the neurite initiation, migration, polarization and differentiation*.

Neuronal migration is a complex sequence of motile and morphogenetic events, in which neurons extend primary

processes and translocate the nucleus into this process. These movements are driven by actin and MTs filaments, the first promotes neuronal migration by propulsive contractions at the cell rear and MTs which are anchored to the centrosome extend the leading process and form a cage-like structure around the nucleus. Cytoskeletal forces in the leading edge can pull the centrosome into the proximal part of the leading process and move the nucleus in the direction of cell migration (22).

Neurite initiation and outgrowth begins with the breakage of the circular shape of new-born neurons by emerging neurites. These newborn neurites are composed by bundled MTs and a growth cone which mediates the pushing and pulling forces that provide to membrane protrusion (23,24).

MT stabilization plays a fundamental role in axon *differentiation* during the neuronal polarization. The increased MTs stability leads to kinesin mediated flow and contributes to determining the future axon formation. The complete mechanism of axon differentiation remains unknown, but internal signals, like centrosome localization, Golgi position and cytoskeleton architecture, could introduce a local imbalance inside the MT network that leads to stabilize MTs in only one of the many neurites (25,26).

During *axonal elongation* the MT cytoskeleton participates in functional interactions with actin and adhesion complex, that with +TIPs can modulate the MT properties and stability (25). In addition to MT polymerization, recent studies found that the translocation of whole MT bundles into the axon contribute to axon elongation, that is presumably generated by molecular motors (27,28).

Dendritic spine morpho dynamic and synapse functioning are linked directly to MT dynamics, in fact, evidences suggest that MTs are associated with transient changes in spine shape, such as the formation and enlargement of the spine. MTs that entered into spines are regulated by the neuronal activity and brain derived neurotrophic factor (BDNF), these MTs with MT dependent motors are responsible to drive postsynaptic cargoes into spines (29).

MTs cytoskeleton is organized in bundles and axonal cross sections are usually composed by 10-100 MTs. In several cell types, MTs are nucleated at the microtubule organizing centre (MTOC), such as the centrosome, but they can be generated even in other different places, such as the Golgi apparatus or along existing MTs, where not all the minus ends are directed towards the MTOC (30,31). In new-born neurons the centrosome first acts as an active MTOC, but with time this activity is completely lost. Super resolution studies and electron microscopy have shown that MTs are not anchored to the centrosome and often in mature neurons there are free ends (**Figure 2**).

Because most MTs do not emerge from MTOC, their relative orientations can be different. Electron microscopy with hook decoration technique showed that MTs orientations in axons and dendrites have two different patterns (32). In axons is possible to observe uniformly plus end out oriented MTs, while in proximal dendrites

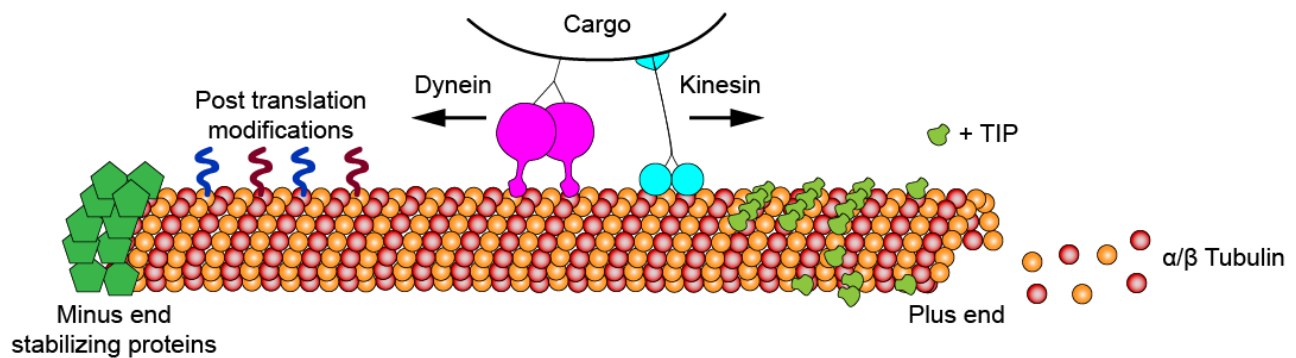


Figure 1. The cartoon illustrates different MAPs that interact with the MT.

the MTs orientations are non-uniformly, in fact MTs are half plus end out and half minus end out oriented.

This different distribution in MTs orientation contributes to the differential trafficking in axons or dendrites (33). The selective presence of minus end out oriented in dendrites allow dyneins to selectively transport cargoes in dendrites. On the other hand, kinesin 1 has been shown to selectively transport cargoes into the axon, where MTs are composed by almost all plus end out oriented (25,34). This separation of duties is possible because kinesin move along the MTs towards the plus end while dynein move to the minus end (35).

Microtubule Associated Proteins

The microtubule dynamics cannot be efficient and determined only by polymerized tubulin, but need specific proteins that interacts with tubulin – the microtubule associated proteins (MAPs). Depending on their role, MAPs can be categorized into motile MAPs, motor proteins that generate movements and forces (36,37); enzymes that cut or depolymerize tubulin (38); nucleators (39); end-binding proteins that bind the minus or plus ends of microtubules (13); and the structural MAPs. While, the first four categories of MAPs are well defined by their functions, the last group bind microtubules to stabilize them, but there is not a clear and broad view on their functions (40).

Structural MAPs are a large category, that includes different proteins all able to decorate the MT cytoskeleton, but only some of them, such as tau, induce microtubule bundling (41,42). A possible mechanism on how MAPs can directly participate in microtubule bundling was recently proposed: MAPs are proteins rich in positive charged amino acids, the abundance of this charges neutralize the negative charges of the C-terminals of tubulins (43). This process reduces the electrostatic repulsion between MTs and allow the bundling them.

In particular, MAP2 is extremely present in brain and its function is directly related to neuronal plasticity. It has multiple isoforms, the high molecular weight (HMW-MAP2), MAP2A and MAP2B selectively expressed in neurons and the low molecular weight (LMW-MAP2), MAP2C and MAP2D expressed in neurons and glia (44,45). MAP2 induce characteristic changes in

microtubule structure, increase the MTOC-independent microtubule polymerization and is a cross-linker of tubulin filaments (46,47). Reduced levels of MAP2, can be compensate by MAP1b, but the deletion of both genes leads to perinatal lethality (47).

Several different MAPs can potentially coexist on one MTs and a big number of binding sites are present on the microtubule surface. MAPs bind the microtubules for different functions, like binding with specific proteins or cross linking of different MTs. Although a common effect of several MAPs is to reduced microtubule tendency to depolymerize, however is important to remember that MAPs are not merely sticked to MTs, but they dynamically bind and unbind MTs.

Microtubules in Neurodegeneration

Several neurodegenerative disorders are characterized by altered axonal transport, that can cause neuronal damages and death. Though different causes can contribute to damage the axonal transport, in many cases appear that transport deficits result from reduced MT stability (48). Here, I review evidences of MT instability in some of the most common neurodegenerative disease, such as Alzheimer's Disease, Parkinson's Disease, traumatic brain injury and amyotrophic lateral sclerosis.

Microtubules dysfunction in Alzheimer's Disease and Tauopathies

Tauopathies are neurodegenerative disorders characterized by the deposition of insoluble fibrils of hyperphosphorylated tau, that are called neurofibrillary tangles (NFTs) and are localized in the neuronal soma or dendrites. Alzheimer disease (AD) is the most notorious disorder among tauopathies, but it is not only due by tau, in fact this disorder is a mixed proteinopathy, where amyloid beta (A β) peptide, α -synuclein and TDP-43 are usually involved.

Tau protein is thought to play a fundamental role in MT properties and functions: the hyperphosphorylation of tau reduces the binding affinity to MT and lead to form insoluble fibrils. It is believed that Tau - mediated toxicity is due to the formation misfolded insoluble fibrils and/or altered properties of MT that result in a release of tau form MT and a subsequent aggregation into inclusions.

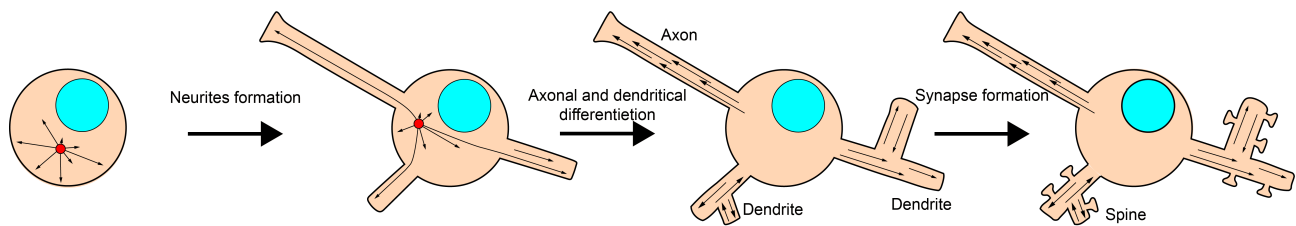


Figure 2. MT changes during neuronal development. After their final division, neurons transit through many developmental stages and the MT cytoskeleton has a crucial role at all the different stages. The MT cytoskeletal organization changes from a radially centrosome-based with largely plus-end out-oriented network to an acentrosomal network with uniform orientations in the axon and mixed orientation in dendrites.

The contribute of tau loss of function in neurodegeneration of tauopathies, is confirmed by observations of reduced number of MT in AD brains and the decreased concentration of acetylated α -tubulin, that is an hallmark of stable MTs. Furthermore, studies on mouse models for NTFs tauopathies revealed abnormalities in MT, such as the reduction in MT concentration, the increased MT dynamicity and reduced axonal transport. These results have led to consider agents that increased MT stability, such as drugs for the treatment of cancer (49), as potential candidates for treatment of AD and tauopathies (50).

Traumatic brain injury

There are many observations that repetitive traumatic brain injuries (TBI) (51) induce chronic traumatic encephalopathy (CTE), characterized by behavioural anomalies and neuronal loss (52). In particular, brains present neurons with diffuse axonal damage, large breakage of the MT cytoskeleton and the loss of axonal transport (53–55). Interestingly, repeated TBI can lead to develop tau pathology that starts to spread out from cortical sulci; this can be explained by the relationship between tauopathies and reduction of MT stability and axonal transport (53,56). Moreover, TBI can outcome in AD or other neurodegenerative symptoms (57). This suggests that MT stabilizing drugs can be effective on the neurodegenerative conditions caused by TBI/CTE. On this way the MT dysfunctions are becoming one of the distinctive features of TBI and on the therapy front, good results are coming from MT stabilizers drugs such as epoD and paclitaxel (58–60)

Parkinson's disease

Parkinson's disease (PD) is a brain disorder which provide locomotor impairments, that is due to the loss of dopaminergic neurons in the substantia nigra pars compacta. Pathological neurons of this region present intra neuronal inclusions of α -synuclein called Lewi bodies. As in AD, there are evidences of MT anomalies in PD brains that probably contribute to neurodegeneration. In fact, the extensive axonal arborization of the dopaminergic neurons of substantia nigra because makes this type of neurons particularly fragile in case of damaged of axonal transport. Studies on the relationship between α -synuclein and MTs revealed that neurons overexpressing α -synuclein present MT dysfunction, compromised MT

dependent trafficking, Golgi fragmentation and neurite degeneration. Interestingly a possible involvement of hyperphosphorylated tau in MT instability was observed in PD models; with the involvement of kinase LRRK2 that is mutated in familiar cases of PD. This protein can phosphorylate tau bound to MTs, reducing the binding of tau with MTs and increasing the free tau inside the cell which can lead to pathology. Furthermore, the increased tau phosphorylation by mutated LRRK2 is probably due to an enhanced binding affinity between mutated LRRK2 and MTs. Moreover, overexpression of LRRK2 in transgenic mouse models with mutation A53T on α -synuclein worsen the pathology and with an acceleration in α -synuclein aggregation, that can be due to the damaged dynamics of MT. Therefore, alterations in MTs stability can cause an increase of both α -synuclein and tau pathology.

Lastly decreased MT stability can also come from mutations on Parkin protein that cause familial PD. Studies on neurons derived from iPSC fibroblasts of patients with mutated Parkin protein showed a reduction in MTs stability and consequently a reduced neurite length and arborization. Notably, the altered morphology of this neurons can be repaired with the administration of pacilitaxel, a MT stabilizing drug (61).

However, action of Parkin protein on MT is not fully understood and interesting it can interact with HDAC6 (62), that can deacetylate MTs, but additional studies are needed to investigate the Parking effect on MT.

Amyotrophic lateral sclerosis

Amyotrophic lateral sclerosis (ALS) is a progressive nervous system disease of motor neurons (63). Why these neurons seem to be the more vulnerable to ALS is not completely clear, but MT instability and deficient axonal transport would be particularly destructive in motor neurons that have a morphology with longest axons in the body. In this way there are evidences that support the involvement of defective axonal transport in ALS (64). For example, dynactin is a protein that works in association with dynein, is very important in retrograde axonal transport, but when mutated in subunit p150glued can cause motor neuron disease and maybe ALS (65). Additionally, 10% of hereditary ALS cases present mutations superoxidase dismutase 1 (SOD1) gene, that participates anterograde mitochondrial transport inaxons (66). Experiments on transgenic mouse models with

SOD1 mutated develop axonal transport deficits before the onset of the neurodegeneration (67,68). In addition, these transgenic mice line present increased MT dynamicity that can be restored on normal levels with nospapine, can restore the axonal transport and decrease the MT turnover, with a reduced cell death (69). Moreover, other studies in ALS mouse models confirmed that mutated SOD1 increase the MT dynamicity, expanding the evidences that mutations in SOD1 perturb the MT homeostasis (70,71).

As mutated SOD1 concerns a little fraction of ALS patients, evidence of altered MT dynamics and axonal transport are needed in non SOD1 ALS models to support the involvement of MTs in ALS. In this way, studies on mouse model for ALS (TDP-43) revealed that mutations on TDP-43, a DNA binding protein, are associated with axonal transport problems (72). TDP-43 is implicated in ALS, in fact it is the main protein found in ubiquitin positive inclusions that are characteristic of ALS pathology. In addition, mouse models TDP-43 have a reduction in mitochondrial motility, that can appear just before the onset of the first symptoms of ALS (73).

Nevertheless, the molecular mechanisms implicated are not fully understood and further experiments will be necessary to understand the molecular cascade that links TDP-43 and SOD1 with MT stability and ALS.

Therapeutic Drugs

As discussed herein, there are several evidences that the axonal transport deficit is involved in numerous neurodegenerative disease and this is probably induced by the altered MT stability. In these way MT stabilizing drugs were identified as potential candidates for treatment of neurodegenerative disease. MT stabilizing drugs, as it is known, can inhibit the cell division and thus are the ideal drugs to work in CNS and interact with neurons. Recent results with epothiloneD (epoD) a MT stabilizer show encouraging benefits in mouse models (74). In particular, different studies showed the efficacy of epoD in reducing the MT hyperdynamicity and neuronal loss. This drug is particularly effective in thapaties and AD (75–77), but significant benefits were noted even for TBI and PD (58,78). However, other drugs were studied in mouse models, such as dictyostatin, this drug have relevant benefits in the CNS, but complications in the gastrointestinal tract and mortality was observed on mouse models (79–82). This show that not all MT stabilizing drugs are equal, and that carefulness and further studies will be necessary to guarantee benefits without major side effects.

Microtubules in Psychiatric Disease

Cytoskeleton dysfunctions have been observed even in several neuropsychiatric disorders such as schizophrenia, major depressive disorder (MDD) and bipolar disorder. The hypothesis that altered MT dynamics leads to a disrupted synaptic connectivity is supported by clinical studies and animal models. Here, I present some findings that connects altered MTs homeostasis with psychiatric diseases.

Tubulin Isozymes

During human brain development various tubulin isozymes are expressed, the different isozymes can influence the structural and interaction properties of the MT and have different affinity with PMT modifications. In particular α_{IA} , β_{II} and β_{III} are the most present tubulin isozymes in the brain, while α_{IB} , α_{IC} , β_I and β_{IVb} that are expressed in the whole body. Altered expression of tubulin isozymes were identified from proteomic studies in rodent models of depression. It has been noted that isolation rodent models have a reduction in α -tubulin expression (83) and rats genetically sensitive to depression have a huge decrease in β_{IIA} and β_V tubulin expression in hippocampus (84). These studies show that reduced α and β tubulin expression in hippocampus is a hallmark of depression in rodents models.

It is possible to observe decreased tubulin isozymes even in humans, for example in patients with schizophrenia or bipolar disorder have a decreased expression of β -tubulin isotype in the prefrontal cortex (85). Coherent with this, gene expression analysis from patients with major depressive disorder, shows that *TUBB4* and *TUBB2C* isozymes are down-regulated in the dorsolateral prefrontal cortex (86). Taken together these data highlight that the expression of tubulin isozymes is significantly altered in clinical and animal models of psychiatric disorders, showing that distorted tubulin homeostasis is a characteristic these circumstances.

Tubulin PTMs

Post translational modifications of tubulin (PTMs) is a powerful mechanism to generate specific microtubule identities (87). These modifications which include acetylation/deacetylation, phosphorylation, tyrosination/detyrosination, glutamylation and polyglycylation create a unique environment for the interaction of specific MAPs to the MTs (88).

Acetylation/deacetylation. Acetylation can be performed on both α and β tubulin residues, where acetyl transferase α TAT and Atat-2 act on the former and Sun acetyltransferase work on β -tubulin (88). On the other hand, deacetylation is performed by histone deacetylase 6 (HDAC6) and nicotine adenine dinucleotide-dependent deacetylase sirtuin-2 (SIRT2) (89).

The role of HDAC inhibitors as antidepressants is well known and it was largely tested on rodent models of depression (90). On this way, behavioural studies conducted on HDAC6 Knockout (KO) mice revealed that these mice express low anxiety, hyperactivity and low depressive phenotype (91). Furthermore, reduced expression of SIRT2 deacetylase is characteristic in rodent models of depression, suggesting that this deacetylase protein can be directly implicated in depressive behaviour (92).

Reduced levels of tubulin acetylation have been observed even in rats after social isolation (83), while they are increased in the hippocampus of rats after exposure to unpredictable chronic mild stress (93). Tubulin acetylation is also diminished after knockdown of *Ulk4* (Unc-51 like kinase-4), a gene that has been funded deleted in

schizophrenia and bipolar disorders(94). Mouse models with *Ulk4* knockdown have reduced neurite length, diminished branching, and agenesis of the corpus callosum. Interestingly also, c-Jun NH2-terminal protein kinase (JNK) activity is reduced in these *Ulk4* knockdown mice (95). JNK is a protein that regulate the MT homeostasis and neurite complexity and it can represent a possible link between *Ulk4* and MT integrity.

All these findings suggest that tubulin acetylation levels are altered in models of schizophrenia and depression. This can be the cause of abnormalities in the development of axons and dendrites and synaptic plasticity. Furthermore, kinases implicated in schizophrenia have a role in the pathway that controls MT stabilization, suggesting a link between pathological symptoms and the loss of cytoskeletal homeostasis.

Phosphorylation. The addition of a phosphate group results in a gain of negative charges that change the chemical properties of tubulin. Phosphorylation is performed on neuronal β III tubulin and on α -tubulin, this mechanism is particularly active during neuronal differentiation and helps the microtubule polymerization (96–98). Phosphorylation of tubulin induces conformational changes of MT, this can change the binding site for stabilizing drugs used in psychiatric disease such as valproate lithium and paliperidone, implying that this modifications are relevant in pathologies (99).

Tyrosination/detyrosination. Tyrosination is performed by tubulin tyrosine ligase (TTL) on α -tubulin; tyrosinated tubulin increase microtubule dynamics while detyrosination enhance microtubule stability, these dynamics are important in axonal extension and transport (88). Detyrosination concerns the removal of Tyr from the C-terminal of α -tubulin to expose a Glu residue. In this way, Glutamylolation is done by tubulin tyrosine ligase-like (TTLL), that add chains of glutamates to the carboxy terminal of tubulin. This happens at high levels usually in brain. Polyglutamylolation influence the surface charges on MTs modifying the binding properties to MAPs and motor proteins (100). It is known that damaged protein transport and the compromised binding of MAPs can contribute to pathology in schizophrenia (101). In fact, problems on the TTLL11 ployglutamylase gene are linked to schizophrenia and bipolar disorder (102,103).

Polyglycylation. This modification is peculiar of cilia and flagella. It can be present on α and β tubulin and the responsible enzymes are the members of the TTL family (104). Glycylation is important in stabilization and motility of ependymal cilia which plate ventricles of the brain (105), but it is interesting to note that in cilia effects of diverse neuropsychiatric risk genes converge (106).

MAPs

MAPs are fine regulators of the microtubule properties and function in neuronal network; therefore an imperfect function of these proteins can give rise to neurodegenerative, developmental and psychiatric disorders (29).

MAPs in Psychiatric Disorders

Dendritic arborization and spine density is directly related with MAPs (29), in fact reduced levels of these can lead to neurological disease (107,108), intellectual disability (109), depression (110,111) and schizophrenia (108). In case of depression the synapse loss damages the feedback loops and the adaptive response for stress (112). Spine loss in schizophrenia is associated with reduced MAP2 (113), suggesting a participation in the spine stabilization, suggesting a role for MT in in spine head stability. Crucial for synaptic disorders is also how MAP2 impact on CREB activity by binding PKA in dendrites (114). CREB controls the expression of BDNF, that is fundamental in synapse and neuronal survival.

Loss of MAP2 immunoreactivity is an hallmark of schizophrenia

In the last twenty years several studies were conducted post-mortem on schizophrenia patients and a common feature of the analysed brains were the reduced immunoreactivity of MAP2 (113). This was localized specifically in hippocampus and prefrontal cortex where it coincides with diminished dendrite ramification. The reduced immunoreactivity noted does not mean reduced MAP2, in fact proteomic analysis on schizophrenic or depressed patients show no altered levels of MAP2 protein (85). Consistent with this MAP2 mRNA is not altered in patients with schizophrenia (115), but the decreased immunoreactivity seems due to PTM of MAP2 (e.g., phosphorylation), that limit the epitope recognition. This modification probably can lead to an altered function of MAP2 and contribute to the typical disorders of psychiatric disease.

MAP6

Like MAP2, MAP6 stabilizes microtubules, binding together the nearby microtubules (116,117). Mice *MAP6* KO present severe symptoms associated with schizophrenia, that can be anxiety, impaired cognition, hyperactivity and social withdrawal (118). In particular, MAP6 deletion damage the cognitive function damaging the synaptic connectivity (118,119). Studies on post-mortem brains evidence that mRNA MAP6 levels are improved in prefrontal cortex of patients with schizophrenia. These studies together suggest an involvement of MAP6 with the onset of the schizophrenia (120), but further study will be necessary to point out the molecular mechanism.

Therapeutic Drugs

These studies indicate that microtubule regulators and PTM of MAPs are altered in psychiatric disorders. Some effects of these modifications can be rescued by the treatment with antidepressant drugs, neurosteroids like microtubule associated protein neurosteroidal pregnenolone (MAPREG), pregnenolone (PREG) and dehydroepiandrosterone (DHEA) were noticed to enhance the neuronal survival and improve long term memory (121). Binding of these neurosteroids that are

synthesized in multiple glial cells (122,123), promotes the neurite growth stimulating the MAP2 effect on MT polymerization (123–126). Neurosteroids improve the neuronal survival and have a neuroprotective effect, they can even stimulate neurogenesis in adult hippocampus improving the long term memory (127–129).

On the other hand, were noted that MT drugs have significant benefits on behaviour. In particular, lithium is a mood stabilizing drug used to treat bipolar disorder (130,131). Studies revealed that the administration of lithium directly inhibit GSK-3, this reduces the phosphorylation of tau and MAP1B protein leading to MT remodelling (132–134). Modification of the cytoskeleton structure may help to stimulate the neuroplasticity in the brain areas interested by the mood disorder like hippocampus and amygdala (135).

Conclusions

As discussed herein, there is a convincing number of evidences that axonal transport troubles are involved in several neurodegenerative and neuropsychiatric disease. This issues in transport can be due in part or whole to the perturbed MT homeostasis, increase or decrease of microtubule stability. The focus of this review has been on how MT variations can alter axonal transport and there is a growing number of studies regarding MT defects in cell cultures or animal models of neurodegenerative or psychiatric disease. These observations have led to experiment MT stabilizing drugs, usually used in the treatment of cancer, on animal models of disease with good results. The challenge now is to develop and test new drugs that can support the treatment of neurodegenerative or psychiatric disease in human patients.

Conflict of interest

The authors declare that there is no conflict of interests regarding the publication of this paper.

References

1. Coles CH, Bradke F. Coordinating neuronal actin-microtubule dynamics. *Curr Biol*. 2015;25(15):R677–91.
2. Sainath R, Gallo G. Cytoskeletal and signaling mechanisms of neurite formation. *Cell Tissue Res*. 2015;359(1):267–78.
3. Mortal S, Iseppon F, Perissinotto A, D'Este E, Cojoc D, Napolitano LMR, et al. Actin waves do not boost neurite outgrowth in the early stages of neuron maturation. *Front Cell Neurosci*. 2017;11:402.
4. Howard J. Molecular motors: structural adaptations to cellular functions. *Nature*. 1997;389(6651):561–7.
5. Akhmanova A, Steinmetz MO. Tracking the ends: a dynamic protein network controls the fate of microtubule tips. *Nat Rev Mol Cell Biol*. 2008;9(4):309–22.
6. Barnes AP, Polleux F. Establishment of axon-dendrite polarity in developing neurons. *Annu Rev Neurosci*. 2009;32:347–81.
7. Kuijpers M, Hoogenraad CC. Centrosomes, microtubules and neuronal development. *Mol Cell Neurosci*. 2011;48(4):349–58.
8. Lipka J, Kuijpers M, Jaworski J, Hoogenraad CC. Mutations in cytoplasmic dynein and its regulators cause malformations of cortical development and neurodegenerative diseases. *Biochem Soc Trans*. 2013;41(6):1605–12.
9. Reiner O, Sapir T. LIS1 functions in normal development and disease. *Curr Opin Neurobiol*. 2013;23(6):951–6.
10. Howard J, Hyman AA. Growth, fluctuation and switching at microtubule plus ends. *Nat Rev Mol Cell Biol*. agosto 2009;10(8):569–74.
11. Alushin GM, Lander GC, Kellogg EH, Zhang R, Baker D, Nogales E. High-resolution microtubule structures reveal the structural transitions in α -tubulin upon GTP hydrolysis. *Cell*. 2014;157(5):1117–29.
12. Brouhard GJ, Rice LM. Microtubule dynamics: an interplay of biochemistry and mechanics. *Nat Rev Mol Cell Biol*. 2018;19(7):451–63.
13. Akhmanova A, Steinmetz MO. Control of microtubule organization and dynamics: two ends in the limelight. *Nat Rev Mol Cell Biol*. 2015;16(12):711–26.
14. Akhmanova A, Hoogenraad CC. Microtubule minus-end-targeting proteins. *Curr Biol*. 2015;25(4):R162–71.
15. Akhmanova A, Hoogenraad CC. Microtubule plus-end-tracking proteins: mechanisms and functions. *Curr Opin Cell Biol*. 2005;17(1):47–54.
16. Dehmelt L, Halpain S. The MAP2/Tau family of microtubule-associated proteins. *Genome Biol*. 2004;6(1):204.
17. Subramanian R, Kapoor TM. Building complexity: insights into self-organized assembly of microtubule-based architectures. *Dev Cell*. 2012;23(5):874–85.
18. Kollman JM, Merdes A, Mourey L, Agard DA. Microtubule nucleation by γ -tubulin complexes. *Nat Rev Mol Cell Biol*. 2011;12(11):709–21.
19. Sharp DJ, Ross JL. Microtubule-severing enzymes at the cutting edge. *J Cell Sci*. 2012;125(11):2561–9.
20. Hirokawa N, Niwa S, Tanaka Y. Molecular motors in neurons: transport mechanisms and roles in brain function, development, and disease. *Neuron*. 2010;68(4):610–38.
21. Hammond JW, Huang C-F, Kaech S, Jacobson C, Banker G, Verhey KJ. Posttranslational modifications of tubulin and the polarized transport of kinesin-1 in neurons. *Mol Biol Cell*. 2010;21(4):572–83.
22. Cooper JA. Cell biology in neuroscience: mechanisms of cell migration in the nervous system. *J Cell Biol*. 2013;202(5):725–34.
23. Cáceres A, Ye B, Dotti CG. Neuronal polarity: demarcation, growth and commitment. *Curr Opin Cell Biol*. 2012;24(4):547–53.
24. Flynn KC, Hellal F, Neukirchen D, Jacob S, Tahirovic S, Dupraz S, et al. ADF/Cofilin-mediated actin retrograde flow directs neurite formation in the developing brain. *Neuron*. 2012;76(6):1091–107.
25. Nakata T, Hirokawa N. Microtubules provide directional cues for polarized axonal transport through interaction with kinesin motor head. *J Cell Biol*. 2003;162(6):1045–55.
26. Nakata T, Niwa S, Okada Y, Perez F, Hirokawa N. Preferential binding of a kinesin-1 motor to GTP-tubulin-rich microtubules underlies polarized vesicle transport. *The J Cell Biol*. 2011;194(2):245–55.
27. Hellal F, Hurtado A, Ruschel J, Flynn KC, Laskowski CJ, Umlauf M, et al. Microtubule stabilization reduces scarring and causes axon regeneration after spinal cord injury. *Science*. 2011;331(6019):928–31.
28. Ruschel J, Hellal F, Flynn KC, Dupraz S, Elliott DA, Tedeschi A, et al. Systemic administration of ephothilone B promotes axon regeneration after spinal cord injury. *Science*. 2015;348(6232):347–52.
29. Hoogenraad CC, Bradke F. Control of neuronal polarity and plasticity – a renaissance for microtubules? *Trends Cell Biol*. 2009;19(12):669–76.
30. Bettencourt-Dias M, Glover DM. Centrosome biogenesis and function: centrosomics brings new understanding. *Nat Rev Mol Cell Biol*. 2007;8(6):451–63.
31. Kapitein LC, Hoogenraad CC. Building the neuronal

- microtubule cytoskeleton. *Neuron*. 2015;87(3):492–506.
32. Baas PW, Lin S. Hooks and comets: The story of microtubule polarity orientation in the neuron. *Dev Neurobiol*. 2011;71(6):403–18.
 33. Kapitein LC, Hoogenraad CC. Which way to go? Cytoskeletal organization and polarized transport in neurons. *Mol Cell Neurosci*. 2011;46(1):9–20.
 34. Kapitein LC, Schlager MA, Kuijpers M, Wulf PS, van Spronsen M, MacKintosh FC, et al. Mixed microtubules steer dynein-driven cargo transport into dendrites. *Curr Biol*. 2010;20(4):290–9.
 35. Lu W, Gelfand VI. Moonlighting motors: kinesin, dynein, and cell polarity. *Trends Cell Biol*. 2017;27(7):505–14.
 36. Hirokawa N, Noda Y, Tanaka Y, Niwa S. Kinesin superfamily motor proteins and intracellular transport. *Nat Rev Mol Cell Biol*. 2009;10(10):682–96.
 37. Bhabha G, Johnson GT, Schroeder CM, Vale RD. How dynein moves along microtubules. *Trends Biochem Sci*. 2016;41(1):94–105.
 38. McNally FJ, Roll-Mecak A. Microtubule-severing enzymes: From cellular functions to molecular mechanism. *J Cell Biol*. 2018;217(12):4057–69.
 39. Roostalu J, Surrey T. Microtubule nucleation: beyond the template. *Nat Rev Mol Cell Biol*. 2017;18(11):702–10.
 40. Bodakuntla S, Jijunam AS, Villablanca C, Gonzalez-Billault C, Janke C. Microtubule-associated proteins: structuring the cytoskeleton. *Trends Cell Biol*. 2019;29(10):804–19.
 41. Kanai Y, Takemura R, Oshima T, Mori H, Ihara Y, Yanagisawa M, et al. Expression of multiple tau isoforms and microtubule bundle formation in fibroblasts transfected with a single tau cDNA. *J Cell Biol*. 1989;109(3):1173–84.
 42. Barlow S, Gonzalez-Garay ML, West RR, Olmsted JB, Cabral F. Stable expression of heterologous microtubule-associated proteins (MAPs) in Chinese hamster ovary cells: evidence for differing roles of MAPs in microtubule organization. *J Cell Biol*. 1994;126(4):1017–29.
 43. Wang Q, Crevenna AH, Kunze I, Mizuno N. Structural basis for the extended CAP-Gly domains of p150glued binding to microtubules and the implication for tubulin dynamics. *Proc Natl Acad Sci U S A*. 2014;111(31):11347–52.
 44. Kalcheva N, Albala J, O'Guin K, Rubino H, Garner C, Shafiq-Zagardo B. Genomic structure of human microtubule-associated protein 2 (MAP-2) and characterization of additional MAP-2 isoforms. *Proc Natl Acad Sci U S A*. 1995;92(24):10894–8.
 45. Matsunaga W, Miyata S, Kiyohara T. Redistribution of MAP2 immunoreactivity in the neurohypophysial astrocytes of adult rats during dehydration. *Brain Res*. 1999;829(1–2):7–17.
 46. Al-Bassam J, Ozer RS, Safer D, Halpain S, Milligan RA. MAP2 and tau bind longitudinally along the outer ridges of microtubule protofilaments. *J Cell Biol*. 2002;157(7):1187–96.
 47. Teng J, Takei Y, Harada A, Nakata T, Chen J, Hirokawa N. Synergistic effects of MAP2 and MAP1B knockout in neuronal migration, dendritic outgrowth, and microtubule organization. *J Cell Biol*. 2001;155(1):65–76.
 48. Roy S, Zhang B, Lee VM-Y, Trojanowski JQ. Axonal transport defects: a common theme in neurodegenerative diseases. *Acta Neuropathol*. 2005;109(1):5–13.
 49. Zhao Y, Mu X, Du G. Microtubule-stabilizing agents: New drug discovery and cancer therapy. *Pharmacol Ther*. 2016;162:134–43.
 50. Tsai RM, Miller Z, Koestler M, Rojas JC, Ljubenkov PA, Rosen HJ, et al. Reactions to multiple ascending doses of the microtubule stabilizer TPI-287 in patients with Alzheimer Disease, progressive supranuclear palsy, and corticobasal syndrome: A randomized clinical trial. *JAMA Neurol*. 2020;77(2):215–24.
 51. Young JS, Hobbs JG, Bailes JE. The impact of traumatic brain injury on the aging brain. *Curr Psychiatry Rep*. 2016;18(9):81.
 52. Saulle M, Greenwald BD. Chronic traumatic encephalopathy: A review. *Rehabil Res Pract*. 2012;2012:816069.
 53. Johnson VE, Stewart W, Smith DH. Axonal pathology in traumatic brain injury. *Exp Neurol*. 2013;246:35–43.
 54. Tang-Schomer MD, Johnson VE, Baas PW, Stewart W, Smith DH. Partial interruption of axonal transport due to microtubule breakage accounts for the formation of periodic varicosities after traumatic axonal injury. *Exp Neurol*. 2012;233(1):364–72.
 55. Tang-Schomer MD, Patel AR, Baas PW, Smith DH. Mechanical breaking of microtubules in axons during dynamic stretch injury underlies delayed elasticity, microtubule disassembly, and axon degeneration. *FASEB J*. 2010;24(5):1401–10.
 56. McKee AC, Alosco ML, Huber BR. Repetitive head impacts and chronic traumatic encephalopathy. *Neurosurg Clin N Am*. 2016;27(4):529–35.
 57. Gardner A, Iverson GL, McCrory P. Chronic traumatic encephalopathy in sport: a systematic review. *Br J Sports Med*. 2014;48(2):84–90.
 58. Brizuela M, Blizzard CA, Chuckowree JA, Dawkins E, Gasperini RJ, Young KM, et al. The microtubule-stabilizing drug Epothilone D increases axonal sprouting following transection injury in vitro. *Mol Cell Neurosci*. 2015;66:129–40.
 59. Cross DJ, Garwin GG, Cline MM, Richards TL, Yarnykh V, Mourad PD, et al. Paclitaxel improves outcome from traumatic brain injury. *Brain Res*. 2015;1618:299–308.
 60. Chuckowree JA, Zhu Z, Brizuela M, Lee KM, Blizzard CA, Dickson TC. The microtubule-modulating drug Epothilone D alters dendritic spine morphology in a mouse model of mild traumatic brain injury. *Front Cell Neurosci*. 2018;12:223.
 61. Ren Y, Jiang H, Hu Z, Fan K, Wang J, Janoschka S, et al. Parkin mutations reduce the complexity of neuronal processes in iPSC-derived human neurons. *Stem Cells*. 2015;33(1):68–78.
 62. Jiang Q, Ren Y, Feng J. Direct binding with histone deacetylase 6 mediates the reversible recruitment of parkin to the centrosome. *J Neurosci*. 2008;28(48):12993–3002.
 63. Masrori P, Damme PV. Amyotrophic lateral sclerosis: a clinical review. *Eur J Neurol*. 2020;27(10):1918–29.
 64. Bercier V, Hubbard JM, Fidelin K, Duroure K, Auer TO, Revenu C, et al. Dynactin1 depletion leads to neuromuscular synapse instability and functional abnormalities. *Mol Neurodegener*. 2019;14(1):27.
 65. Puls I, Jonnakuty C, LaMonte BH, Holzbaur ELF, Tokito M, Mann E, et al. Mutant dynactin in motor neuron disease. *Nat Genet*. 2003;33(4):455–6.
 66. Moller A, Bauer CS, Cohen RN, Webster CP, De Vos KJ. Amyotrophic lateral sclerosis-associated mutant SOD1 inhibits anterograde axonal transport of mitochondria by reducing Miro1 levels. *Hum Mol Genet*. 2017;26(23):4668–79.
 67. Zhang B, Tu P, Abtahian F, Trojanowski JQ, Lee VM-Y. Neurofilaments and orthograde transport are reduced in ventral root axons of transgenic mice that express human SOD1 with a G93A mutation. *J Cell Biol*. 1997;139(5):1307–15.
 68. Williamson TL, Cleveland DW. Slowing of axonal transport is a very early event in the toxicity of ALS-linked SOD1 mutants to motor neurons. *Nat Neurosci*. 1999;2(1):50–6.
 69. Fanara P, Banerjee J, Hueck RV, Harper MR, Awada M, Turner H, et al. Stabilization of hyperdynamic microtubules is neuroprotective in amyotrophic lateral sclerosis. *J Biol Chem*. 2007;282(32):23465–72.
 70. Kleele T, Marinković P, Williams PR, Stern S, Weigand EE, Engerer P, et al. An assay to image neuronal microtubule dynamics in mice. *Nat Commun*. 2014;5(1):4827.
 71. Huai J, Zhang Z. Structural properties and interaction partners of familial ALS-associated SOD1 mutants. *Front Neurol*. 2019;10:527.
 72. Cohen TJ, Lee VMY, Trojanowski JQ. TDP-43 functions and pathogenic mechanisms implicated in TDP-43 proteinopathies. *Trends Mol Med*. 2011;17(11):659–67.
 73. Magrané J, Cortez C, Gan W-B, Manfredi G. Abnormal

- mitochondrial transport and morphology are common pathological denominators in SOD1 and TDP43 ALS mouse models. *Hum Mol Genet.* 2014;23(6):1413–24.
74. Brunden KR, Yao Y, Potuzak JS, Ferrer NI, Ballatore C, James MJ, et al. The characterization of microtubule-stabilizing drugs as possible therapeutic agents for Alzheimer's disease and related tauopathies. *Pharmacol Res.* 2011;63(4):341–51.
 75. Brunden KR, Zhang B, Carroll J, Yao Y, Potuzak JS, Hogan A-ML, et al. Etoposide D improves microtubule density, axonal integrity, and cognition in a transgenic mouse model of tauopathy. *J Neurosci.* 2010;30(41):13861–6.
 76. Zhang B, Carroll J, Trojanowski JQ, Yao Y, Iba M, Potuzak JS, et al. The microtubule-stabilizing agent, Etoposide D, reduces axonal dysfunction, neurotoxicity, cognitive deficits, and Alzheimer-like pathology in an interventional study with aged tau transgenic mice. *J Neurosci.* 2012;32(11):3601–11.
 77. Barten DM, Fanara P, Andorfer C, Hoque N, Wong PYA, Husted KH, et al. Hyperdynamic microtubules, cognitive deficits, and pathology are improved in tau transgenic mice with low doses of the microtubule-stabilizing agent BMS-241027. *J Neurosci.* 2012;32(21):7137–45.
 78. Killinger BA, Moszczynska A. Etoposide D prevents binge methamphetamine-mediated loss of striatal dopaminergic markers. *J Neurochem.* 2016;136(3):510–25.
 79. Brunden KR, Gardner NM, James MJ, Yao Y, Trojanowski JQ, Lee VM-Y, et al. MT-stabilizer, dictyostatin, exhibits prolonged brain retention and activity: potential therapeutic implications. *ACS Med Chem Lett.* 2013;4(9):886–9.
 80. Makani V, Zhang B, Han H, Yao Y, Lassalas P, Lou K, et al. Evaluation of the brain-penetrant microtubule-stabilizing agent, dictyostatin, in the PS19 tau transgenic mouse model of tauopathy. *Acta Neuropathol Commun.* 2016;4(1):106.
 81. Ballatore C, Brunden KR, Huryn DM, Trojanowski JQ, Lee VM-Y, Smith AB. Microtubule stabilizing agents as potential treatment for Alzheimer's Disease and related neurodegenerative tauopathies. *J Med Chem.* 2012;55(21):8979–96.
 82. Brunden KR, Trojanowski JQ, Smith AB, Lee VM-Y, Ballatore C. Microtubule-stabilizing agents as potential therapeutics for neurodegenerative disease. *Bioorg Med Chem.* 2014;22(18):5040–9.
 83. Bianchi M, Shah AJ, Fone KCF, Atkins AR, Dawson LA, Hebdreder CA, et al. Fluoxetine administration modulates the cytoskeletal microtubular system in the rat hippocampus. *Synapse.* 2009;63(4):359–64.
 84. Piubelli C, Carboni L, Becchi S, Mathé AA, Domenici E. Regulation of cytoskeleton machinery, neurogenesis and energy metabolism pathways in a rat gene-environment model of depression revealed by proteomic analysis. *Neuroscience.* 2011;176:349–80.
 85. Prabakaran S, Swatton JE, Ryan MM, Huffaker SJ, Huang JT-J, Griffin JL, et al. Mitochondrial dysfunction in schizophrenia: evidence for compromised brain metabolism and oxidative stress. *Mol Psychiatry.* 2004;9(7):684–97, 643.
 86. Kang HJ, Voleti B, Hajszan T, Rajkowska G, Stockmeier CA, Licznernski P, et al. Decreased expression of synapse-related genes and loss of synapses in major depressive disorder. *Nat Med.* 2012;18(9):1413–7.
 87. Verhey KJ, Gaertig J. The tubulin code. *Cell Cycle.* 2007;6(17):2152–60.
 88. Magiera MM, Janke C. Post-translational modifications of tubulin. *Curr Biol.* 2014;24(9):R351–4.
 89. Hubbert C, Guardiola A, Shao R, Kawaguchi Y, Ito A, Nixon A, et al. HDAC6 is a microtubule-associated deacetylase. *Nature.* 2002;417(6887):455–8.
 90. Fuchikami M, Thomas A, Liu R, Wohleb ES, Land BB, DiLeone RJ, et al. Optogenetic stimulation of infralimbic PFC reproduces ketamine's rapid and sustained antidepressant actions. *Proc Natl Acad Sci U S A.* 2015;112(26):8106–11.
 91. Fukada M, Hanai A, Nakayama A, Suzuki T, Miyata N, Rodriguiz RM, et al. Loss of deacetylation activity of Hdac6 affects emotional behavior in mice. *PLOS ONE.* 2012;7(2):e30924.
 92. Liu R, Dang W, Du Y, Zhou Q, Jiao K, Liu Z. SIRT2 is involved in the modulation of depressive behaviors. *Sci Rep.* 2015;5(1):8415.
 93. Yang C, Wang G, Wang H, Liu Z, Wang X. Cytoskeletal alterations in rat hippocampus following chronic unpredictable mild stress and re-exposure to acute and chronic unpredictable mild stress. *Behav Brain Res.* 2009;205(2):518–24.
 94. Lang B, Pu J, Hunter I, Liu M, Martin-Granados C, Reilly TJ, et al. Recurrent deletions of ULK4 in schizophrenia: a gene crucial for neurogenesis and neuronal motility. *J Cell Sci.* 2014;127(3):630–40.
 95. Coffey ET. Nuclear and cytosolic JNK signalling in neurons. *Nat Rev Neurosci.* 2014;15(5):285–99.
 96. Alexander JE, Hunt DF, Lee MK, Shabanowitz J, Michel H, Berlin SC, et al. Characterization of posttranslational modifications in neuron-specific class III beta-tubulin by mass spectrometry. *Proc Natl Acad Sci U S A.* 1991;88(11):4685–9.
 97. Matten WT, Aubry M, West J, Maness PF. Tubulin is phosphorylated at tyrosine by pp60c-src in nerve growth cone membranes. *J Cell Biol.* 1990;111(5):1959–70.
 98. Greenberger L.M., Loganzo F. (2008) Destabilizing Agents. In: Fojo T. (eds) *The Role of Microtubules in Cell Biology, Neurobiology, and Oncology.* Cancer Drug Discovery and Development. Humana Press. https://doi.org/10.1007/978-1-59745-336-3_10
 99. Corena-McLeod M, Walss-Bass C, Oliveros A, Villegas AG, Ceballos C, Charlesworth CM, et al. New model of action for mood stabilizers: phosphoproteome from rat prefrontal cortex synaptoneurosomal preparations. *PLOS ONE.* 2013;8(5):e52147.
 100. Janke C. The tubulin code: Molecular components, readout mechanisms, and functions. *J Cell Biol.* 2014;206(4):461–72.
 101. Ikegami K, Heier RL, Taruishi M, Takagi H, Mukai M, Shimma S, et al. Loss of α -tubulin polyglutamylation in ROSA22 mice is associated with abnormal targeting of KIF1A and modulated synaptic function. *Proc Natl Acad Sci U S A.* 2007;104(9):3213–8.
 102. Rajkumar AP, Christensen JH, Mattheisen M, Jacobsen I, Bache I, Pallesen J, et al. Analysis of t(9;17)(q33.2;q25.3) chromosomal breakpoint regions and genetic association reveals novel candidate genes for bipolar disorder. *Bipolar Disord.* 2015;17(2):205–11.
 103. Fullston T, Gabb B, Callen D, Ullmann R, Woollatt E, Bain S, et al. Inherited balanced translocation t(9;17)(q33.2;q25.3) concomitant with a 16p13.1 duplication in a patient with schizophrenia. *Am J Med Genet B Neuropsychiatr Genet.* 2011;156(2):204–14.
 104. Fukushima N, Furuta D, Hidaka Y, Moriyama R, Tsujiuchi T. Post-translational modifications of tubulin in the nervous system. *J Neurochem.* 2009;109(3):683–93.
 105. Bosch Grau M, Gonzalez Curto G, Rocha C, Magiera MM, Marques Sousa P, Giordano T, et al. Tubulin glycosylases and glutamylases have distinct functions in stabilization and motility of ependymal cilia. *J Cell Biol.* 2013;202(3):441–51.
 106. Marley A, Zastrow M von. A simple cell-based assay reveals that diverse neuropsychiatric risk genes converge on primary cilia. *PLOS ONE.* 2012;7(10):e46647.
 107. Blanpied TA, Ehlers MD. Microanatomy of dendritic spines: emerging principles of synaptic pathology in psychiatric and neurological disease. *Biol Psychiatry.* 2004;55(12):1121–7.
 108. Penzes P, Cahill ME, Jones KA, VanLeeuwen J-E, Woolfrey KM. Dendritic spine pathology in neuropsychiatric disorders. *Nat Neurosci.* 2011;14(3):285–93.
 109. Kaufmann WE, MacDonald SM, Altamura CR. Dendritic cytoskeletal protein expression in mental retardation: an immunohistochemical study of the neocortex in Rett

- syndrome. *Cereb Cortex*. 2000;10(10):992–1004.
110. Duman EA, Canli T. Influence of life stress, 5-HTTLPR genotype, and SLC6A4 methylation on gene expression and stress response in healthy Caucasian males. *Biol Mood Anxiety Disord*. 2015;5:2.
 111. Varidaki A, Mohammad H, Coffey ET. Chapter 5 - Molecular Mechanisms of Depression. In: Frodl T, curatore. *Systems Neuroscience in Depression* [Internet]. San Diego: Academic Press; 2016 [citato 5 febbraio 2021]. pag. 143–78. Disponibile su: <https://www.sciencedirect.com/science/article/pii/B9780128024560000054>
 112. Gold PW. The organization of the stress system and its dysregulation in depressive illness. *Mol Psychiatry*. 2015;20(1):32–47.
 113. Shelton MA, Newman JT, Gu H, Sampson AR, Fish KN, MacDonald ML, et al. Loss of microtubule-associated protein 2 immunoreactivity linked to dendritic spine loss in schizophrenia. *Biol Psychiatry*. 2015;78(6):374–85.
 114. Harada A, Teng J, Takei Y, Oguchi K, Hirokawa N. MAP2 is required for dendrite elongation, PKA anchoring in dendrites, and proper PKA signal transduction. *J Cell Biol*. 2002;158(3):541–9.
 115. Law AJ, Weickert CS, Hyde TM, Kleinman JE, Harrison PJ. Reduced spinophilin but not microtubule-associated protein 2 expression in the hippocampal formation in schizophrenia and mood disorders: molecular evidence for a pathology of dendritic spines. *Am J Psychiatry*. 2004;161(10):1848–55.
 116. Bosc C, Cronk JD, Pirollet F, Watterson DM, Haiech J, Job D, et al. Cloning, expression, and properties of the microtubule-stabilizing protein STOP. *Proc Natl Acad Sci U S A*. 1996;93(5):2125–30.
 117. Lefèvre J, Savarin P, Gans P, Hamon L, Clément M-J, David M-O, et al. Structural basis for the association of MAP6 protein with microtubules and its regulation by calmodulin. *J Biol Chem*. 2013;288(34):24910–22.
 118. Fournet V, Schweitzer A, Chevarin C, Deloulme J-C, Hamon M, Giros B, et al. The deletion of STOP/MAP6 protein in mice triggers highly altered mood and impaired cognitive performances. *J Neurochem*. 2012;121(1):99–114.
 119. Gozes I. Microtubules, schizophrenia and cognitive behavior: preclinical development of davunetide (NAP) as a peptide-drug candidate. *Peptides*. 2011;32(2):428–31.
 120. Shimizu H, Iwayama Y, Yamada K, Toyota T, Minabe Y, Nakamura K, et al. Genetic and expression analyses of the STOP (MAP6) gene in schizophrenia. *Schizophr Res*. 2006;84(2–3):244–52.
 121. Plassart-Schiess E, Baulieu E-E. Neurosteroids: recent findings. *Brain Res Brain Res Rev*. 2001;37(1):133–40.
 122. Tsutsui K, Ukena K, Usui M, Sakamoto H, Takase M. Novel brain function: biosynthesis and actions of neurosteroids in neurons. *Neurosci Res*. 2000;36(4):261–73.
 123. Fontaine-Lenoir V, Chambraud B, Fellous A, David S, Duchossoy Y, Baulieu E-E, et al. Microtubule-associated protein 2 (MAP2) is a neurosteroid receptor. *Proc Natl Acad Sci U S A*. 2006;103(12):4711–6.
 124. Cardounel A, Regelson W, Kalimi M. Dehydroepiandrosterone protects hippocampal neurons against neurotoxin-induced cell death: mechanism of action. *Proc Soc Exp Biol Med*. 1999;222(2):145–9.
 125. Marx CE, Jarskog LF, Lauder JM, Gilmore JH, Lieberman JA, Morrow AL. Neurosteroid modulation of embryonic neuronal survival in vitro following anoxia. *Brain Res*. 2000;871(1):104–12.
 126. Murakami K, Fellous A, Baulieu E-E, Robel P. Pregnenolone binds to microtubule-associated protein 2 and stimulates microtubule assembly. *Proc Natl Acad Sci U S A*. 2000;97(7):3579–84.
 127. Roberts E, Bologna L, Flood JF, Smith GE. Effects of dehydroepiandrosterone and its sulfate on brain tissue in culture and on memory in mice. *Brain Res*. 1987;406(1):357–62.
 128. Flood JF, Morley JE, Roberts E. Memory-enhancing effects in male mice of pregnenolone and steroids metabolically derived from it. *Proc Natl Acad Sci U S A*. 1992;89(5):1567–71.
 129. Karishma KK, Herbert J. Dehydroepiandrosterone (DHEA) stimulates neurogenesis in the hippocampus of the rat, promotes survival of newly formed neurons and prevents corticosterone-induced suppression. *Eur J Neurosci*. 2002;16(3):445–53.
 130. Drago A, Crisafulli C, Sidoti A, Calabrò M, Serretti A. The microtubule-associated molecular pathways may be genetically disrupted in patients with Bipolar Disorder. Insights from the molecular cascades. *J Affect Disord*. 2016;190:429–38.
 131. Beurel E, Song L, Jope RS. Inhibition of glycogen synthase kinase-3 is necessary for the rapid antidepressant effect of ketamine in mice. *Mol Psychiatry*. 2011;16(11):1068–70.
 132. Goold RG, Owen R, Gordon-Weeks PR. Glycogen synthase kinase 3beta phosphorylation of microtubule-associated protein 1B regulates the stability of microtubules in growth cones. *J Cell Sci*. 1999;112(19):3373–84.
 133. Grimes CA, Jope RS. CREB DNA binding activity is inhibited by glycogen synthase kinase-3β and facilitated by lithium. *J Neurochem*. 2001;78(6):1219–32.
 134. Bélanger D, Farah CA, Nguyen MD, Lauzon M, Cornibert S, Leclerc N. The projection domain of MAP2b regulates microtubule protrusion and process formation in Sf9 cells. *J Cell Sci*. 2002;115(7):1523–39.
 135. Cole AR. Glycogen synthase kinase 3 substrates in mood disorders and schizophrenia. *The FEBS Journal*. 2013;280(21):5213–27.

RNA-seq analysis reveals that oleic acid exerts anti-inflammatory effects via modulating cell cycle in Raw264.7 cells

Taoyu LI^{1,#}, Wanli LIANG^{2,#}, Xiaojun LI¹, Wei Kevin ZHANG^{1,2}

1 School of Pharmaceutical Sciences, South-Central University for Nationalities, No.182, Minzu Avenue, Wuhan, 430074, China.

2 Bioland Laboratory, (Guangzhou Regenerative Medicine and Health Guangdong Laboratory), Guangzhou, 510700, China.

these authors contributed equally to this work.

*Correspondence: wkzhang81@139.com

<https://doi.org/10.37175/stemedicine.v2i6.83>

ABSTRACT

Background: Lipopolysaccharide (LPS), a structural and protective compound primarily found in ordinary benign bacteria, could induce pro-inflammatory effect in a macrophage cell line Raw264.7 cells. Additionally, we previously showed that oleic acid (OA) possessed apoptotic effect in mouse-originated Raw264.7 cells as well.

Methods: Cellular and molecular methods including flow cytometry and Western blot as well as bioinformatic methods including RNA-seq and analysis.

Results: We demonstrated that OA could alleviate LPS-activated inflammatory effects, including apoptosis and secretion of cytokines via the modulation of cell cycle process. Further analysis revealed that OA reduced the LPS-elevated expression of p21, but not p16.

Conclusion: Our investigation has provided detailed information on LPS stimulation and OA remission in Raw264.7 cells, and laid solid foundation for the potential pharmaceutical application of OA as an anti-inflammatory agent.

Keywords: Oleic acid · Lipopolysaccharide · Cell cycle control · p21Cip1/Waf1 · Transcriptome

Introduction

Our immune system is made up of at least two parts: the faster but more general innate immunity, and the slower but more specific adaptive immunity. The innate immunity is important for us to defend against microbial pathogens, and stands as the first line of defense in our body. Macrophages are a group of innate immune cells playing essential roles in the host defense process and maintenance of tissue homeostasis (1). Macrophages are capable of engulfing particles to engage as a primary function in phagocytosis (2). In addition, our immune

system could also be altered by macrophages through the production and secretion of various cellular factors including interferons, interleukins, growth factors and lipid mediators (3). Meanwhile, macrophages is also important for tissue repair processes as well (4). Due to its importance in the immunity, the functions and regulations of macrophages have been extensively studied.

Lipopolysaccharide (LPS), made up of lipids and sugar, is a structural and protective compound primarily found in ordinary benign bacteria, which, once presented in the bloodstream after microbial invasion, could drive sudden activation of macrophages and subsequent release of inflammatory mediators (5). It has been well established that, upon the treatment of LPS, macrophages could elicit pathogenic inflammatory responses (6) by the production and release of immune regulated enzymes such as nitric oxide synthases (iNOS) and cyclooxygenase-2 (COX-2),

Received: Feb 22, 2021; Accepted: Mar 6, 2021.

© The Author(s). 2020 This is an **Open Access** article distributed under the terms of the Creative Commons License (<http://creativecommons.org/licenses/by/4.0/>) which permits unrestricted use, distribution, and reproduction in any medium or format, provided the original work is properly cited.

as well as cytokines and chemokines such as interleukin-1 β (IL-1 β), tumor necrosis factor (TNF)- α , and IL-6 (7). Due to the observations of dysregulated inflammatory responses in many inflammatory disorders including asthma, rheumatoid arthritis and other autoimmune diseases (8), it would be quite beneficial to study the regulation of LPS-activated inflammatory response in macrophages.

Various investigations indicated that fatty acids exhibited inhibitory effect on cytokine production in LPS-stimulated human monocytes and Raw264.7 cells (9-12). Additional study showed that fatty acids exerted anti-inflammatory effects via blocking transcriptional factors including nuclear factor κ B (NF- κ B) (13), and suppressing the function of mitogen-activated protein kinases (MAPKs) (14). Meanwhile, we previously reported that unsaturated fatty acids extracted from Chrysanthemum, including linoleic acid and linolenic acid, induced apoptosis of Kupffer cells, a type of specific tissue-resided macrophages in the liver (15).

Therefore, we intended to investigate the detailed mechanism of oleic acid (OA) in suppressing both LPS-induced apoptotic and pro-inflammatory effects in Raw264.7 macrophages in this study by combining biochemistry and bio-informatics approaches.

Materials and Methods

Reagents

The DMEM (10569-044) basic medium supplemented with fetal bovine serum (12484-010) was obtained from Gibco (Thermo Fisher Scientific, Waltham, MA, USA). The cell counting kit-8 (CCK-8; BestBio, BB4202) was used for cell survival assay. Antibodies were provided either by CST or Abcam. LPS (L8880) and bovine serum albumin (BSA; A8010) were obtained from Solarbio (Beijing, China) and OA (HY-N1446) were from MedChemExpress. The OA storage solution was prepared by dissolving OA in a BSA solution (15 mM) at the concentration of 100 mM. OA working solution was obtained via a dilution of the storage solution in a ratio of 1:50. Cell cycle analysis kit (40301ES60) and apoptosis detection kit (40302ES60) were obtained from Yeasen.

Cell culture and cell survival assay

Mouse macrophages (Raw264.7, GDC0143) were delivered from the China Center for Type Culture Collection (Wuhan, China). Normally macrophages were maintained in a CO₂ incubator at 37 °C. Cell morphology was monitored under a microscope (Eclipse Ti, Nikon Inc) and imaged with a DI-RS2 camera (Nikon Inc).

The CCK-8 assay was used to monitor the cytotoxicity of LPS and OA to Raw264.7 cells. Briefly, Raw264.7 cells with a density of approximately 1×10^5 cells/mL were placed into 96-well plates, and then treated separately for 24 h. Next, CCK-8 was added for an incubation of 2 h. Absorbance at 450 nm were monitored using an Infinite 200 PRO system (Tecan Group Ltd., Maennedorf,

Switzerland). All experiments were done in triplicates and conducted independently for three times at least. A set of control wells without cells was included in each plate.

Apoptosis monitoring via flow cytometry

Raw264.7 cells with a density of 1×10^6 cells were placed into a well of the six-well plate. After incubated with indicated treatments, cells were washed and aspirated in 1 mL PBS. Later 5 μ L Annexin-V-FITC were suspended in 400 μ L binding buffer and directly added to a well for 15 mins at 4 °C. Finally, 10 μ L PI buffer was incubated for 5 mins. Flow cytometry (Guava System; Merck, Germany) was used for the detection.

qPCR performance and analysis

Total RNA was extracted from indicated treatment of Raw264.7 cells using TRIzol reagent (Invitrogen) and reversely transcribed with a PrimeScript RT reagent kit (Takara, Dalian, China). The transcriptional expression levels were analyzed by qPCR using Thermal Cycler Dice Real Time System (Takara, Shiga, Japan). Ordinary conditions with $\Delta\Delta$ Ct method were used during the performance of qPCR. Each data were represented from triplicates. GAPDH for each experiment was monitored and employed as an internal control.

The primer sets used in mouse-sourced Raw264.7 cells were:

For COX-2 (*ptgs2*),

forward, 5'-GCGACATACTCAAGCAGGAGCA-3' and reverse, 5'-AGTGGTAACCGCTCAGGTGTTG-3';

For iNOS (*nos2*),

forward, 5'-GAGACAGGGAAGTCTGAAGCAC-3' and reverse, 5'-CCAGCAGTAGTTGCTCCTCTTC-3';

For β -catenin (*ctnnb1*),

forward, 5'-GTTTCGCCTTCATTATGGACTGCC-3' and reverse, 5'-ATAGCACCTGTTCCCGCAAAG-3';

For F4/80 (*agrel*),

forward, 5'-CGTGTGTTGTTGGTGGCACTGTGA-3' and reverse, 5'-CCACATCAGTGTTCAGGAGAC-3';

For CD68 (*cd68*),

forward, 5'-GGCGGTGGAATACAATGTGTCC-3' and reverse, 5'-AGCAGGTCAAGGTGAACAGCTG-3';

For CD206 (*mrc1*),

forward, 5'-GTTACCTGGAGTGATGGTTCTC-3' and reverse, 5'-AGGACATGCCAGGGTCACCTTT-3'.

Detection of protein expressions

After treatments as indicated, cells were harvested and the total protein concentration was determined. After that, lysates of cells were fractionated with either 10% or 12.5% SDS-PAGE gels and transferred to PVDF membranes (IPVH00010; Millipore Corporation, MA, USA). After blockage with 5% non-fat milk, the membranes were blotted with antibodies against the following proteins: caspase-3 (1:1000, 9662S, CST), PARP (1:500, 9542S, CST), iNOS (1:500, ab15323, Abcam), COX-2 (1:1000, ab169782, Abcam), p16 (1:1000, 18769S, CST), p21 (1:500, 2947S, CST)

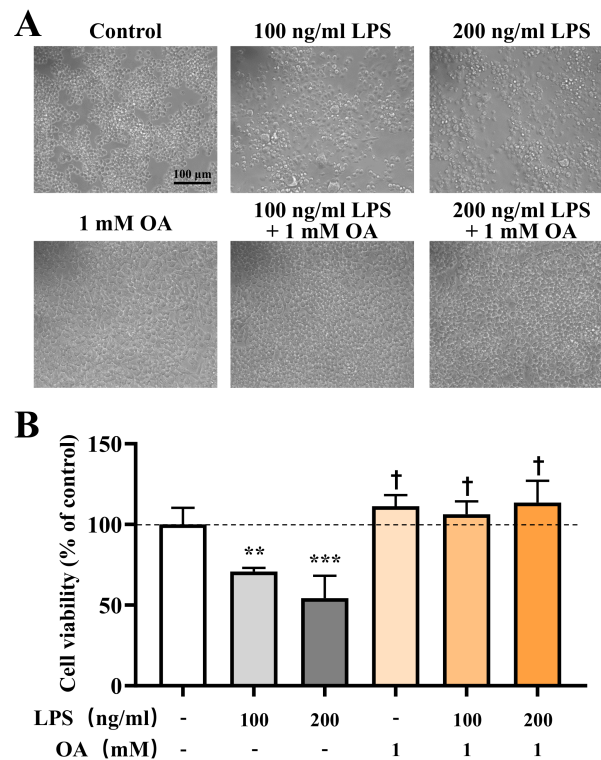


Figure 1. OA induces loss of Raw264.7 cells. (A) Representative images of cells under different treatments. Scale bar, 100 μ m. (B) Summary of cell viability after 24 h treatment of various conditions. ** and *** represented significant different from the control with a $p < 0.01$ and 0.001 , respectively. † represented no significant difference comparing with the control. The dashed line indicated 100% viability.

and β -actin (1:1000, 4970S, CST) at 4 °C overnight. After that, the blot was washed thrice with TBST solution and followed by the incubation with a secondary antibody (1:2000, goat anti-rabbit or goat anti-mouse, A21010 or A21020, Abbkine, USA) for 1 h at room temperature. A developer and fixing solution were used for visualization of protein bands. ImageJ and Microsoft Excel were used for quantification and analysis of the protein bands.

RNA-sequencing and analysis

RNA samples were collected and used for the construction of cDNA libraries by an Illumina Truseq™ RNA sample prep kit (Illumina, CA, USA). To summarize, cDNA was prepared and reversely transcribed in a double-stranded manner. After that, they were ligated and amplified before the assessment and quantitation of the library. Cluster generation of loads of a single mRNA-sequencing library was performed on the Cluster Station. Sequence-by-synthesis single reads of 54-base-length using the Hiseq2000 Truseq SBS Kit (v3-HS, Illumina) were generated on the HiSeq X system. TPM and FPKM matrix were calculated from the read count matrix. FPKMs were mainly used for the analysis among samples while less biased TPMs were used for further analysis on gene expressions. Gene expression between compared groups with $\log_2FC > 1$ and $p < 0.05$ was considered as significantly different. The Venn diagram was composed at the following website: <https://www.venndiagram.net/venn-diagram-and-sets.html>. The David resources version 6.8 was utilized for the performance of GO enrichment at

the following website: <https://david.ncifcrf.gov>.

Cell cycle phase identification

Raw264.7 cells were plated at the density of 105 in a 35-mm dish and treated with either LPS or OA for 24 h. Later on, cells were detached and washed twice with PBS, and subsequently fixed overnight at 4 °C in 75% ethanol. After removal of ethanol by centrifugation, cells were re-suspended and incubated for 30 min in PBS with 10 μ g/mL of RNase A at 37 °C, and then stained with PI (50 μ g/mL). The fluorescence was measured by a flow cytometric Guava System (Merck, Germany). Cellular multiplets were excluded. Histograms of DNA content were determined by the fractions of the population in cell cycle.

Statistical analysis

Results were normally indicated as means \pm standard error of the mean (SEM). One-way or two-way ANOVA followed by a Tukey's post-hoc test or a Bonferroni post-test as indicated were performed using Microsoft Excel software. Statistical significance was identified with a p value < 0.05 .

Results

OA treatment alleviates inflammatory responses to LPS in Raw264.7 cells

To test the effect of OA treatment on LPS-induced

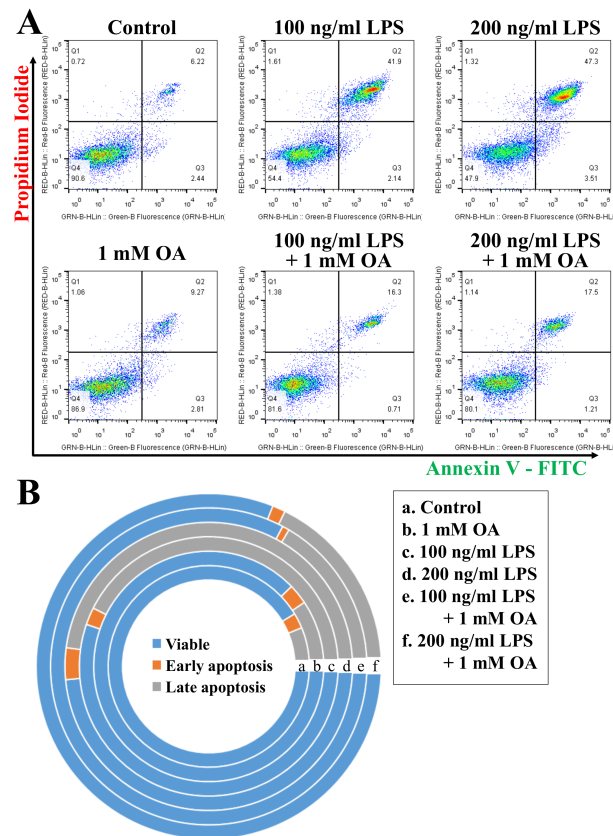


Figure 2. OA treatment alleviates LPS-induced apoptosis in Raw264.7 cells. (A) Flow cytometry analysis of annexin V / PI staining in Raw264.7 cells after various treatments. The proportions of cells were included in each quadrant. (B) Summary of (A) on double staining.

inflammatory responses in Raw264.7 cells, 1 mM OA was added to the culture medium in the presence or absence of LPS treatment (100 and 200 ng/mL for 24 h). As shown in **Figure 1**, the overall morphology and cell viability were greatly alleviated in the OA-treated groups, comparing with LPS treatment alone, suggesting that OA treatment could tranquilize the inflammatory response of Raw264.7 cells to LPS treatment. Comparatively, it is also worth noting that OA treatment alone possessed neither morphological effects nor reduction in viability of Raw264.7 cells. Further flow cytometry analysis confirmed the effect of OA treatment on LPS-induced apoptosis in Raw264.7 cells as demonstrated in **Figure 2**. Interestingly, 1 mM OA treatment was sufficient to nearly abolish the apoptotic effect of 200 ng/mL LPS treatment. However, since 100 ng/mL LPS treatment was far more than enough to illustrate the effect of OA treatment, we therefore used only 100 ng/mL LPS throughout the rest of our investigation.

Additionally, further analysis on both the mRNA and protein levels also revealed the same trends, as illustrated in **Figure 3**. OA treatment greatly reduced the elevated levels of inflammatory effectors and markers, COX-2 (ptgs2) and iNOS (nos2), by the treatment of LPS. Moreover, OA was also effective in decreasing the elevated expression level of β -catenin (ctnb1), the

regulatory protein in the Wnt signaling. Meanwhile, inflammation-related surface markers of Raw264.7 cells during LPS treatment, such as F4/80, CD68 and CD206, were all sensitive to OA treatment. Western blot also demonstrated that apoptosis-related proteins caspase-3 and PARP were sensitive to OA treatment as well. These evidences further strengthened the notion that OA treatment could alleviate inflammatory responses in LPS-stimulated Raw264.7 cells.

RNA-seq analysis reveals a drastic mRNA expression profile change

To comprehensively study the effects of OA treatment on LPS-treated Raw264.7 cells, transcriptome analysis was conducted for the Control group, the LPS (LPS treatment alone) group, and the LPS/OA (LPS plus OA treatment) group. **Figure 4** showed the general correlation and component analysis results. As could be seen, gene profiles with changed expression levels were quite different among the three groups. However, the pattern change of the LPS group was the most significant (with a correlation of 0.92), while the correlation increased to 0.94 between the LPS/OA group and either the LPS or the Control group, suggesting that OA treatment restored, at least, part of the gene expression profiles from the LPS group to the Control group.

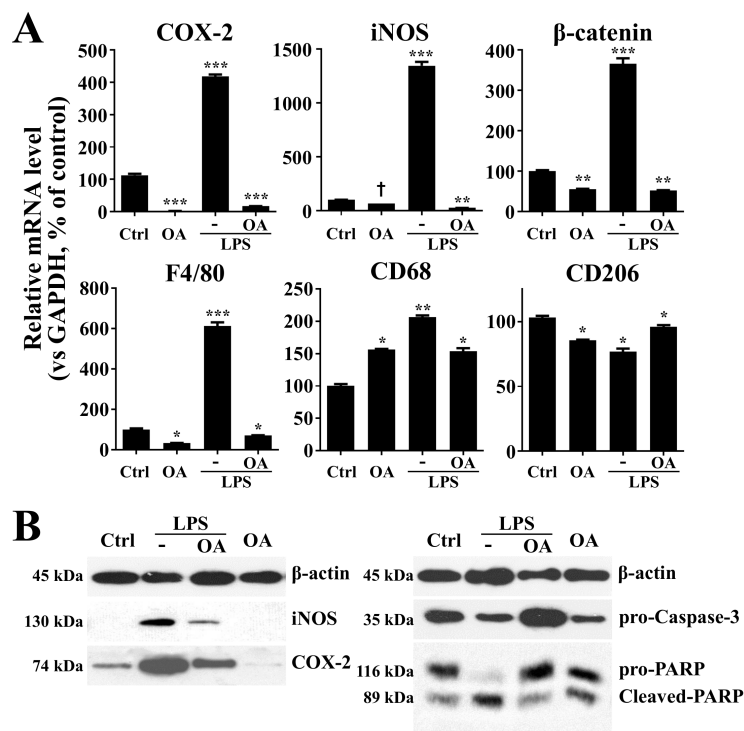


Figure 3. OA treatment alleviates the expression of various factors in the mRNA and/or protein levels. (A) qPCR revealed that OA treatment reduced the expression of inflammatory related factors elevated by LPS. *, **, and *** represent significant different from the control with a $p < 0.05$, 0.01 and 0.001 , respectively. † represented no significant difference comparing with the control. (B) Western blot analysis on the expression levels of various proteins. The molecular weight of each protein was indicated at the left side of the blot.

After a closer look at the expression profiles of the known factors and effectors involved in the inflammation process, many of them increased after LPS treatment, but restored in the presence of OA, as shown in **Figure 5A**. To better separate the expression profiles, genes were categorized into four groups by their behavior: LPS up-regulated, LPS down-regulated, LPS/OA up-regulated and LPS/OA down-regulated genes. Venn diagram was drawn based on the above-mentioned categorization, as illustrated in **Figure 5B**. Primarily, 748 genes located in the LPS up-regulated and LPS/OA down-regulated regions, while 716 genes located in the LPS down-regulated and LPS/OA up-regulated regions (**Figure 5C**). We assumed that most of genes potentially involved should fall into these two categories due to the pattern of changes we observed previously. It was also important to note that 0 could be seen in the Venn diagram since one gene could not be categorized as both LPS down-regulated and up-regulated in the LPS group or likewise in the LPS/OA group. Otherwise, non-zero value occupied these zero would be a sign of defect in the RNA-seq result.

OA treatment modulates cell-cycle related genes to counteract LPS's effect

To further clarify involved genes in OA treatment, genes from the aforementioned four categories were collected for GO enrichment analysis. Results were illustrated in **Figure 6A**, genes that are involved in inflammation-related biological processes fell into three of four categories. While in LPS down-regulated and LPS/OA

up-regulated category (with 716 genes), cell cycle and mitosis were the most enriched biological processes, suggesting a close relationship between these genes and cell cycle control. More importantly, as depicted in **Figure 6B**, 70 out of 119 genes that were related with any of three processes including cell cycle, cell division and mitotic nuclear division, fell into the cross point, suggesting that OA treatment indeed affected the cell cycle control of Raw264.7 cells. Some of the genes and their expression levels were shown in **Figure 6C**, and among them aurora kinase a (*aurka*, mitotic serine/threonine kinase), cyclin A2 (*ccna2*, controls both checkpoint at the G1/S and the G2/M transition), cyclin B2 (*ccnb2*, essential for G2/M transition) and cyclin-dependent kinase 1 (*cdk1*, promotes G1/S and G2/M transition) were known key modulators of the cell cycle.

OA treatment affects cell cycle control via p21 but not p16 in Raw264.7 cells

To confirm our observations in the RNA-seq analysis, cell cycle states of Raw264.7 cells were monitored by flow cytometry. As demonstrated in **Figure 7A** and **B**, LPS treatment significantly decreased the G2 phase population while increased the G0/G1 phase population of Raw264.7 cells. However, OA treatment restored these changes, suggesting that OA treatment indeed recovered the phase population. Further Western blot results demonstrated that p21, instead of p16, were the potential upstream regulator of cell cycle control in the effect of OA on LPS treatment, as shown in **Figure 7C**. This further strengthened the

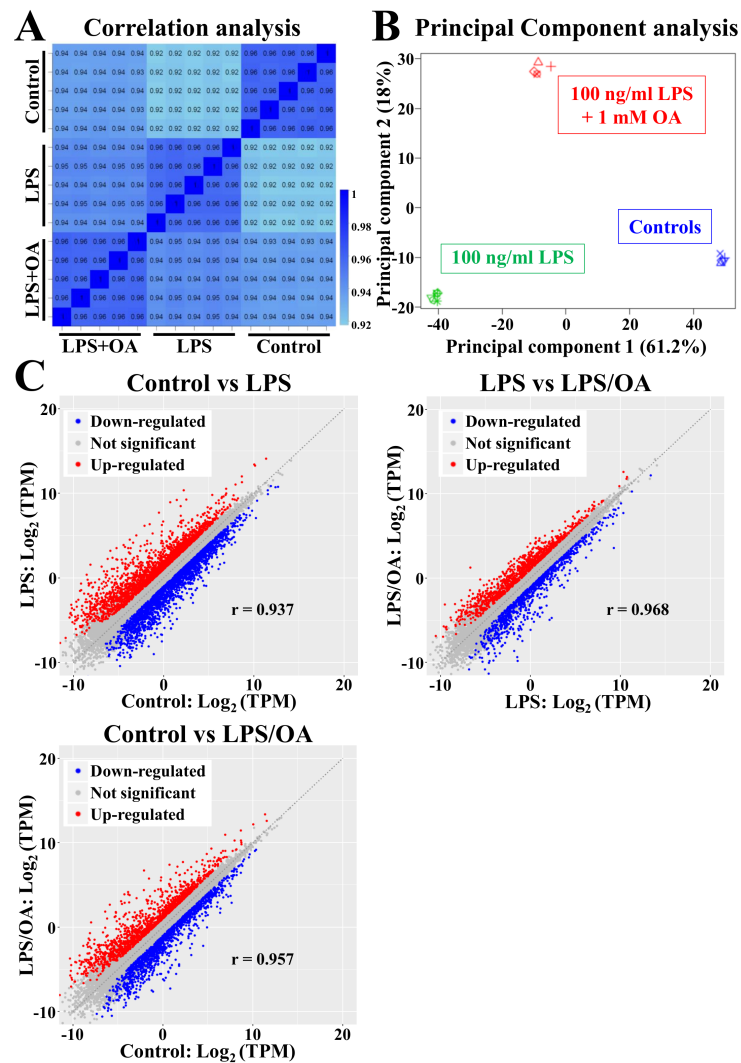


Figure 4. RNA-seq analysis reveals different gene expression profiles in the control, LPS, and LPS/OA groups. (A) Correlation analysis of RNA-seq results. The color of the block indicated the correlation co-efficient. (B) Principle component analysis of the RNA-seq results. (C) Volcano plot of the RNA-seq results. Blue dots indicated expression of down-regulated genes while red dots indicated expression of up-regulated genes. The correlation co-efficient (r) between compared groups was indicated in each image.

notion that OA could restore LPS-induced inflammatory effect via cell cycle control in Raw264.7 cells.

Discussion

In this study, cellular and molecular as well as bioinformatic methods including flow cytometry, qPCR and Western blot were used to verify the detailed mechanism of OA's inhibitory effect on LPS-activated Raw264.7 cells. But before any conclusion could be drawn, several points need to be discussed. Firstly, Raw264.7 cells are a well-established cell model for macrophages. Hence our results here might possess the potential to be extrapolated into other types of macrophages, for instance, microglia in the central nervous system, sinus histiocytes at lymph nodes, pulmonary alveolus, and intestine macrophages in the gastrointestinal tract, which could widen the potential application of OA, or even other fatty acids, in our body, as being proposed previously (16). However, as mentioned

previously (17), the polymorphic feature of Raw264.7 cells, which contain more than one phenotype individually within this cell lineage, would probably compromise the significance of the current study. Meanwhile, the low apoptotic rate by LPS treatment revealed in **Figures 1** and **2**, and the low inhibitory rate of cell cycle in **Figure 7** might be explained largely by this specific feature of Raw264.7 cells as well. Therefore, more investigations on other *in vitro* and *in vivo* systems and/or on other types of fatty acids should be conducted to confirm the phenomenon uncovered in the current study.

Secondly, it has been shown that OA is abundant in olive oil (809.53–1045.52 $\mu\text{g/g}$), which is available and recommended for everyday life (18). Hence, it would be quite meaningful to study the potential pharmacological usage of OA. Various proteins and signaling pathways, including matrix metalloproteinase-9 (19), focal adhesion kinase (20), free fatty acid receptor 1 and free fatty acid receptor 4 (21), mTOR signaling (22), PI3K/AKT

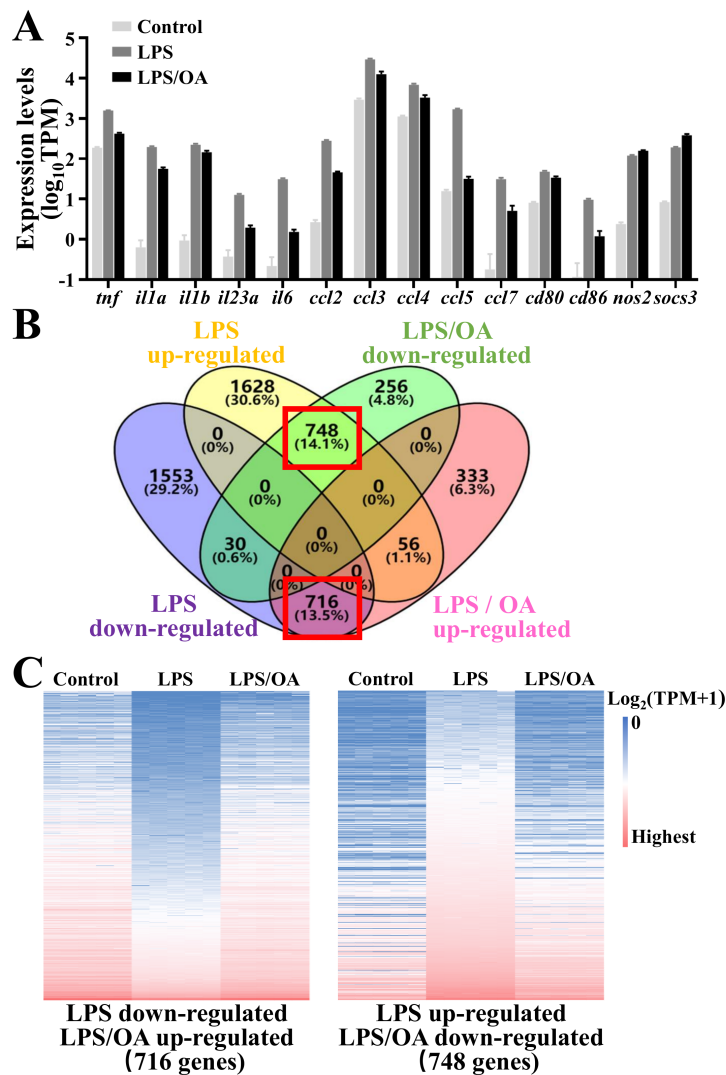


Figure 5. OA treatment partly recovers altered gene expression induced by LPS. (A) Averaged expressions of inflammation-related genes in the RNA-seq analysis. (B) Venn diagram of the RNA-seq results. Red rectangles indicated place of interests. The percentage of gene enclosed in each catalog was enclosed in the bracket. (C) Ordered expression profiles of genes involved in the red rectangles in B. The color of the block indicated expression level of the sample in the form of $\log_2(\text{TPM}+1)$.

signaling (23), etc., have been implicated to be modulated upon the treatment of OA in many different cells and tissues. Meanwhile, as stated in the introduction, investigations also implicated the efficacy of fatty acid treatment on the inhibitory effect in the immune system or in macrophages in particular. However, investigation at the whole transcriptional scale was still insufficient in this very topic. In our study here, RNA-seq analysis was performed in the attempt to acquire more information, and results showed that OA restored the expressions of a large quantities of genes altered by LPS treatment, leaving only a small portion unchanged. Moreover, by combining the results in the LPS group and the LPS/OA group, we successfully narrowed down the target of change into cell cycle process. It was also interesting to note that the mitosis process was also altered and restored by LPS and OA, respectively. This piece of evidence further strengthened the notion that OA was capable

of overturning the pro-inflammatory effect of LPS in macrophages.

Thirdly, p21, sometimes named as p21Cip1/Waf1, is also known as CDK-interacting protein 1, which not only participates in the control of cell cycle process but also is involved in tumor suppression (24). In addition, p21 has been proposed to be a biomarker for cancer stem cells due to their associations. As shown in the current study, OA could reduce the expression of p21 evoked by LPS treatment, which would further highlight the therapeutic potential of OA in cancer treatment. Multiple recent studies illustrated the anti-cancer ability of OA or other fatty acids (25-27), which were quite consistent with the current investigation. However, whether p21 was involved or modulated in this anti-cancer ability still needed to be illustrated. Furthermore, p21 has been shown to be one of the downstream factor of p53 signaling. Here in this study, we observed no significant change in the expression of

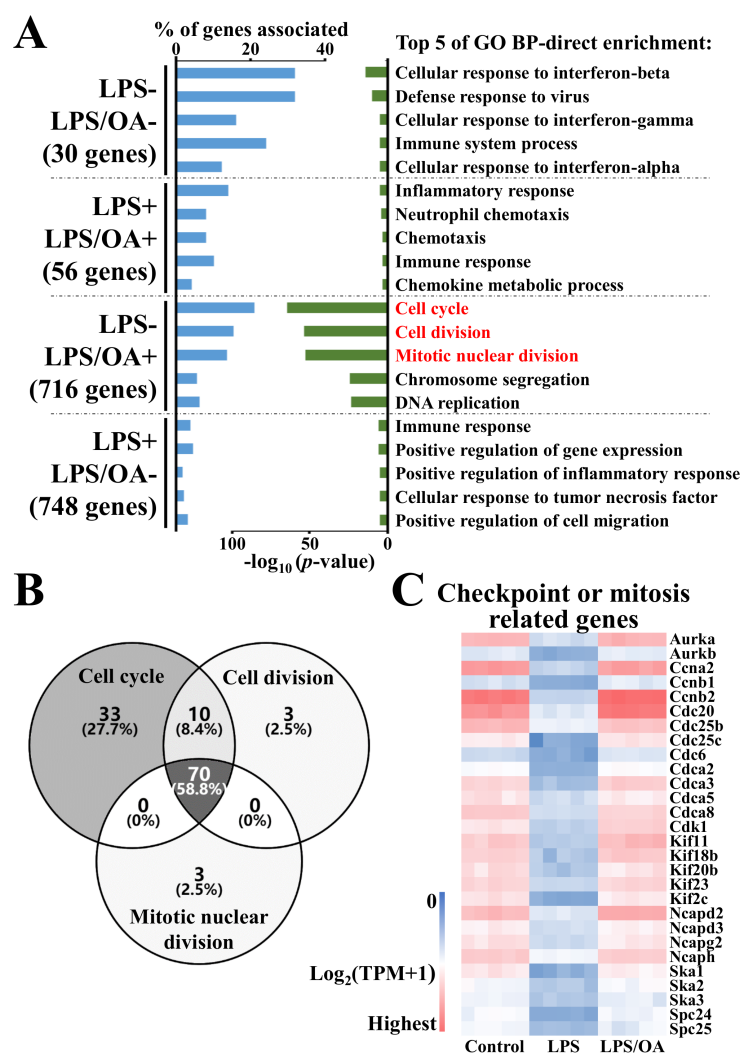


Figure 6. Cell cycle related process is the most obvious in GO analysis of the RNA-seq results. (A) List of top 5 enriched processes in the GO analysis. Red color highlighted processes with the most p value in the analysis. (B) Venn diagram of genes related with the three most enriched processes including cell cycle, cell division, mitotic nuclear division. The percentage of gene enclosed in each catalog was enclosed in the bracket. (C) Expression profiles of checkpoint and/or mitosis related genes.

p53 mRNA in RNA-seq analysis. However, transcriptional change was not the only way for p53 to perform its physiological or pathological functions. Changes in other stages such as post-translational modification and subcellular localization might as well be important for the function of p53. Therefore, it would be plausible to anticipate changes of p53 function after the treatment of OA.

Last but not least, no obvious effect was seen in cells under the OA alone treatment. This suggested that the modulation of cell cycle by OA treatment was limited in the LPS treatment condition. This could be explained partly by the relative low expression levels of p21 before LPS treatment. Alternatively, the internalization and accumulation rate of OA in different states of cells might also be a contributing factor for the ineffectiveness of OA towards unstimulated macrophages.

Conclusion

In a word, in murine macrophage Raw264.7 cells, we have demonstrated that OA could alleviate LPS-stimulated inflammatory effect, via the inhibition of p21 and modulation of the cell cycle.

Conflict of interest

The authors declare that they have no conflicts of interest to disclose.

Funding

This work was supported by the National Natural Science Foundation of China (31400705).

Supplementary Information

The supplemental material can be downloaded online at: <https://stemedicine.org/index.php/stem/article/view/83>

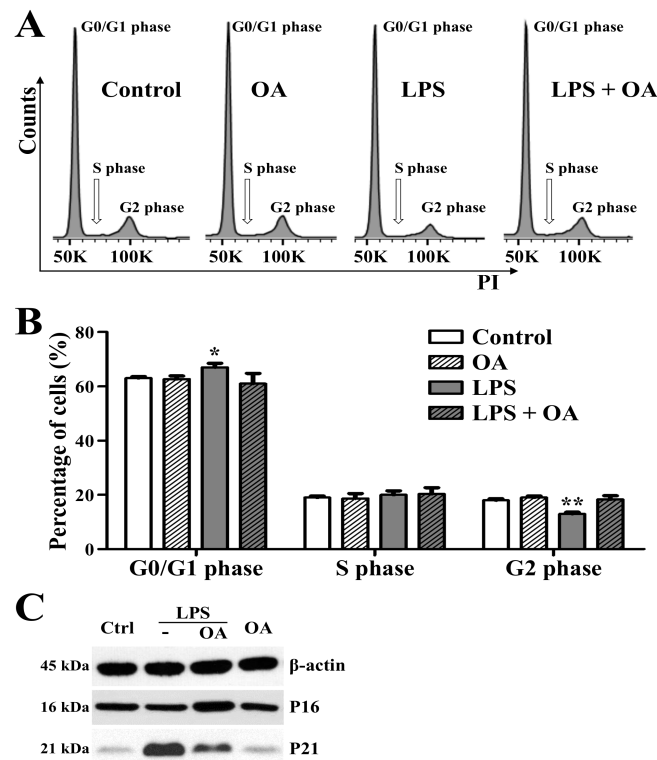


Figure 7. p21 but not p16 controls the alteration of cell cycle process in Raw264.7 cells under LPS or OA treatments. (A) Flow cytometry analysis revealed the increase of G0/G1 phase and the reduction of G2 phase. (B) Summary of A. (C) Western blot analysis revealed that the expression of p16 remained steady while the expression of p21 changed significantly. The molecular weight of each protein was indicated at the left side of the blot.

References

- Galli G, Saleh M. Immunometabolism of macrophages in bacterial infections. *Front Cell Infect Microbiol.* 2020;10:607650.
- Liang WL, Xiao L, Gu HW, Li XJ, Li YS, Zhang WK, et al. Solid lipid nanoparticle induced apoptosis of macrophages via a mitochondrial-dependent pathway in vitro and in vivo. *Int J Nanomedicine.* 2019;14:3283-95.
- Bonnardel J, Guilliams M. Developmental control of macrophage function. *Curr Opin Immunol.* 2018;50:64-74.
- Netea MG, Dominguez-Andres J, Barreiro LB, Chavakis T, Divangahi M, Fuchs E, et al. Defining trained immunity and its role in health and disease. *Nat Rev Immunol.* 2020;20(6):375-88.
- MacMicking J, Xie QW, Nathan C. Nitric oxide and macrophage function. *Annu Rev Immunol.* 1997;15:323-50.
- Guha M, Mackman N. LPS induction of gene expression in human monocytes. *Cell Signal.* 2001;13(2):85-94.
- Rod-In W, Monmai C, Shin IS, You S, Park WJ. Neutral lipids, glycolipids, and phospholipids, isolated from Sandfish (*Arctoscopus japonicus*) eggs, exhibit anti-inflammatory activity in LPS-stimulated RAW264.7 cells through NF-kappaB and MAPKs pathways. *Mar Drugs.* 2020;18(9).
- Xie Y, Meijer AH, Schaaf MJM. Modeling inflammation in zebrafish for the development of anti-inflammatory drugs. *Front Cell Dev Biol.* 2020;8:620984.
- Novak TE, Babcock TA, Jho DH, Helton WS, Espat NJ. NF-kappa B inhibition by omega -3 fatty acids modulates LPS-stimulated macrophage TNF-alpha transcription. *Am J Physiol Lung Cell Mol Physiol.* 2003;284(1):L84-9.
- Babcock TA, Helton WS, Hong D, Espat NJ. Omega-3 fatty acid lipid emulsion reduces LPS-stimulated macrophage TNF-alpha production. *Surg Infect (Larchmt).* 2002;3(2):145-9.
- Zhao G, Etherton TD, Martin KR, Vanden Heuvel JP, Gillies PJ, West SG, et al. Anti-inflammatory effects of polyunsaturated fatty acids in THP-1 cells. *Biochem Biophys Res Commun.* 2005;336(3):909-17.
- Weldon SM, Mullen AC, Loscher CE, Hurley LA, Roche HM. Docosahexaenoic acid induces an anti-inflammatory profile in lipopolysaccharide-stimulated human THP-1 macrophages more effectively than eicosapentaenoic acid. *J Nutr Biochem.* 2007;18(4):250-8.
- Si TL, Liu Q, Ren YF, Li H, Xu XY, Li EH, et al. Enhanced anti-inflammatory effects of DHA and quercetin in lipopolysaccharide-induced RAW264.7 macrophages by inhibiting NF-kappaB and MAPK activation. *Mol Med Rep.* 2016;14(1):499-508.
- Lo CJ, Chiu KC, Fu M, Chu A, Helton S. Fish oil modulates macrophage P44/P42 mitogen-activated protein kinase activity induced by lipopolysaccharide. *JPEN J Parenter Enteral Nutr.* 2000;24(3):159-63.
- Liang WL, Wen Y, Huang F, Hu Q, Li XJ, Zhang WK, et al. Chrysanthemum ethanol extract induced loss of Kupffer cells via the mitochondria-dependent apoptotic pathway. *Food Funct.* 2020;11(10):8866-77.
- Sunesson K, Lindahl J, Chamli Harsmar S, Soderberg G, Lindqvist D. Inflammatory Depression-Mechanisms and Non-Pharmacological Interventions. *Int J Mol Sci.* 2021;22(4).
- Kong L, Smith W, Hao D. Overview of RAW264.7 for osteoclastogenesis study: Phenotype and stimuli. *J Cell Mol Med.* 2019;23(5):3077-87.
- Donovan MG, Selmin OI, Stillwater BJ, Neumayer LA, Romagnolo DF. Do olive and fish oils of the mediterranean diet have a role in triple negative breast cancer prevention and therapy? An exploration of evidence in cells and animal models. *Front Nutr.* 2020;7:571455.
- Soto-Guzman A, Navarro-Tito N, Castro-Sanchez L, Martinez-Orozco R, Salazar EP. Oleic acid promotes MMP-9

- secretion and invasion in breast cancer cells. *Clin Exp Metastasis*. 2010;27(7):505-15.
20. Navarro-Tito N, Soto-Guzman A, Castro-Sanchez L, Martinez-Orozco R, Salazar EP. Oleic acid promotes migration on MDA-MB-231 breast cancer cells through an arachidonic acid-dependent pathway. *Int J Biochem Cell Biol*. 2010;42(2):306-17.
 21. Marcial-Medina C, Ordonez-Moreno A, Gonzalez-Reyes C, Cortes-Reynosa P, Perez Salazar E. Oleic acid induces migration through a FFAR1/4, EGFR and AKT-dependent pathway in breast cancer cells. *Endocr Connect*. 2019;8(3):252-65.
 22. Wu J, Wu Q, Li JJ, Chen C, Sun S, Wang CH, et al. Autophagy mediates free fatty acid effects on MDA-MB-231 cell proliferation, migration and invasion. *Oncol Lett*. 2017;14(4):4715-21.
 23. Hardy S, Langelier Y, Prentki M. Oleate activates phosphatidylinositol 3-kinase and promotes proliferation and reduces apoptosis of MDA-MB-231 breast cancer cells, whereas palmitate has opposite effects. *Cancer Res*. 2000;60(22):6353-8.
 24. Xiao BD, Zhao YJ, Jia XY, Wu J, Wang YG, Huang F. Multifaceted p21 in carcinogenesis, stemness of tumor and tumor therapy. *World J Stem Cells*. 2020;12(6):481-7.
 25. Hirata Y, Inoue A, Suzuki S, Takahashi M, Matsui R, Kono N, et al. trans-Fatty acids facilitate DNA damage-induced apoptosis through the mitochondrial JNK-Sab-ROS positive feedback loop. *Sci Rep*. 2020;10(1):2743.
 26. Li H, Yao Q, Min L, Huang S, Wu H, Yang H, et al. The combination of two bioactive constituents, lactoferrin and linolenic acid, inhibits mouse xenograft esophageal tumor growth by downregulating lithocholytaurine and inhibiting the JAK2/STAT3-related pathway. *ACS Omega*. 2020;5(33):20755-64.
 27. Wang T, Dou Y, Lin G, Li Q, Nie J, Chen B, et al. The anti-hepatocellular carcinoma effect of Brucea javanica oil in ascitic tumor-bearing mice: The detection of brusatol and its role. *Biomed Pharmacother*. 2021;134:111122.

MicroRNA-4284 inhibits colon cancer epithelial-mesenchymal transition by down-regulating Perilipin 5

Xiaofei MIAO, Zengyao LI, Ye ZHANG*, Tong WANG*

Department of General Surgery, Nanjing Medical University Affiliated Wuxi people's Hospital, Wuxi, Jiangsu Province, China.

*Correspondence: aanti@163.com; zhangye2002520@aliyun.com
<https://doi.org/10.37175/stemedicine.v2i6.85>

ABSTRACT

Background: MicroRNA (miR) has been suggested in the development of several types of cancer; yet, the exact function of miR-4284 in colon cancer remains elusive.

Methods: MiR-4284 expression was assessed in normal colon cell line CCD-18Co, and HT-29 and SW480 cell lines representing human colon cancer. Potential target gene of miR-4284 was predicted using TargetScanHuman, and experimentally verified using luciferase report assay. Wound-healing, cell invasion and attachment were evaluated to determine the effect of miR-4284 on the migration, invasion, and metastatic properties of colon cancer cell lines. Expression of epithelial-mesenchymal transition (EMT) phenotypic protein hallmarks, including N-cadherin, E-cadherin, as well as Vimentin, was also evaluated.

Results: MiR-4284 was significantly decreased in colon cancer cell lines, and Perilipin 5 (PLIN5) was found to be directly targeted by miR-4284. Ectopic expression of miR-4284 significantly reduced endogenous expression level of PLIN5 in colon cancer cell lines, suppressing migration, invasion, and metastatic phenotypes. In addition, re-introducing miR-4284 reversed the expression profile of EMT markers.

Conclusion: Our findings for the first time identify miR-4284 as an anti-tumor miRNA in colon cancer, which acts to reduce PLIN5 and inhibit EMT, leading to inhibited colon cancer tumorigenesis. These results highlight the potential of miR-4284 as a therapeutic target in metastatic colon cancer.

Keywords: MicroRNA-4284 · Colon cancer · Perilipin 5 · Tumorigenesis · Epithelial-mesenchymal transition

Introduction

Owing to its lethality, colon cancer causes a significant number of human deaths across the globe. In 2017, approximately 0.1 million new colon cancer cases were reported in US alone (1). Generally, colon cancer treatment includes surgery, chemotherapy and/or radiotherapy (2). However, due to severe side effects of colon cancer chemotherapy, the life quality of the patients is badly impaired (3). Hence, identification of safer drugs and potent therapeutic targets may help to resolve the

problem and enable the efficient management of colon cancer.

MicroRNAs (miRNAs, miRs), a subset of non-coding RNAs that can target mRNAs with complementary sequences and result in translational degradation and/or inhibition (4), are vital players in the proliferation, differentiation, and survival of cells. In 1993, a small RNA was discovered as the first miRNA, transcribed from the lin-4 locus of *Caenorhabditis elegans* (5). Seven years later, let-7, the first mammalian miRNA, was identified (6). Those two key findings sparked a number of genomic studies, which demonstrated extensive transcription of non-coding RNAs, including miRNAs (7, 8).

The capacity of certain miRNAs to target several mRNAs critically modulated in disease states inspires promising therapeutic candidates (miRNA mimics) or

Received: Mar 2, 2021; Accepted: Mar 16, 2021.

© The Author(s). 2020 This is an **Open Access** article distributed under the terms of the Creative Commons License (<http://creativecommons.org/licenses/by/4.0/>) which permits unrestricted use, distribution, and reproduction in any medium or format, provided the original work is properly cited.

targets (anti-miRs) (1, 9-11). In the context of colon cancer, one novel mature microRNA, miR-4284, has been seldom studied. While in other types of human cancers, miR-4284 is frequently involved. For instance, in gastric cancer, miR-4284 was found to promote tumorigenicity by targeting ten-eleven translocation 1 (12). Up-regulating miR-4284 in human glioblastoma could inhibit the viability and induce apoptosis of cancer stem-like cells (13). In clear cell papillary renal cell carcinoma, miR-4284 was shown to be one of the down-regulated miRNAs in a miRNA profiling study (14). Of interest to our study, recently in a similar miRNA profiling investigation among a panel of radioresistant prostate cancer cells, miR-4284 was among the most significantly dysregulated miRNAs (15).

In the present study, we sought to uncover the function of miR-4284 in human colon cancer and elucidate its potential molecular target, as well as the signaling pathway(s) involved in its action.

Materials and Methods

Cell lines

HT-29 and SW480 cells (both human colon cancer cell lines), and CCD-18Co cells (a human normal colon cell line) were acquired from the American Type Culture Collection (ATCC). Cells were maintained in complete RPMI-1640 medium (Hyclone; GE Healthcare) with 10% fetal bovine serum (FBS; Gibco), 100 U/ml penicillin and 100 µg/ml streptomycin, at 37 °C in a humidified atmosphere containing 5% CO₂.

MicroRNA assays

mirVana miRNA negative control (4464061) and hsa-miR-4284 mirVana miRNA mimic (MC17194) were both purchased from Thermo Fisher Scientific (Waltham, MA, USA). Transfection of cells was conducted according to the provided protocols. Following transfection, cultures were kept for another 48 h before any further experiment.

Luciferase reporter assay

The potential miR-4284 binding site at the 3'-untranslated region (3'-UTR) of Perilipin 5 (PLIN5) was inserted at the downstream of the firefly luciferase open reading frame (ORF) driven by a CMV promoter in a pCMV-Firefly Luc vector (16156; Thermo Fisher Scientific). Luciferase construct containing mutated 3'-UTR was prepared with a standard overlap-extension protocol. To determine the luciferase activity, HT-29 or SW480 cells in a 24-well plate (5×10^4 per well) were co-transfected with 200 ng

of wild-type or mutant luciferase constructs, and 400 ng of hsa-miR-4284 or negative control, using Lipofectamine 2000 (Invitrogen). After 48 h, cells were harvested and assessed using the Luc-Screen Extended-Glow Luciferase Reporter Gene Assay System (Thermo Fisher Scientific), following provided protocols.

RNA extraction and quantitative real time polymerase chain reaction (qRT-PCR)

Extraction of total mRNA was performed with mirVana miRNA Isolation Kit (Thermo Fisher Scientific). The miR-4284 expression level was assessed by miRNA-specific TaqMan Pri-miRNA Assay (Hs04227316_pri; Thermo Fisher Scientific) and normalized by RNU48 Control miRNA Assay (001006; Thermo Fisher Scientific). 1 µg of total RNA was prepared for reverse-transcription using Superscript II First-Strand Synthesis kit (Thermo Fisher Scientific) at the manufacturer's recommendation. Levels of GAPDH mRNA were used for normalization. Primers used in the current study are presented in **Table 1**.

Western blot

Cells were plated in 6-well plates at 1×10^6 cells/well density with 2 ml completed RPMI-1640 medium. 24 h following transfection with hsa-miR-4284 or negative control, total protein was prepared with RIPA buffer (150 mM NaCl, 50 mM Tris-HCl pH 7.4, 1 mM EDTA, 1% sodium deoxycholate, 1% Triton X-100, 0.1% sodium dodecyl sulfate (SDS), and protease inhibitors). Protein quantity was assessed by the BCA assay. Proteins of equal amounts were resolved using SDS-PAGE and then transferred onto a nitrocellulose membrane with the semi-dry transfer unit (Bio-Rad Laboratories). Next, the membrane was incubated in blocking buffer (phosphate buffer saline (PBS) plus 0.1% Tween-20) with 5% nonfat milk for 20 min, followed by hybridization with primary antibodies at 4 °C overnight. Primary antibody against PLIN5 was purchased from Proteintech (#26951-1-AP; Wuhan, China), antibodies against N-cadherin (ab18203), E-cadherin (ab76055), Vimentin (ab92547), and GAPDH (ab181602) were all commercially available from Abcam (Cambridge, MA, USA). After washes in blocking buffer, membranes were hybridized with HRP-conjugated secondary antibody (Thermo Fisher Scientific) for 1 h at ambient temperature before visualization with Luminata Forte Western HRP Substrate (EMD Millipore).

Wound-healing assay

Cells (1×10^5) transfected with hsa-miR-4284 or miRNA

Table 1. Primers used for RT-PCR.

Gene	Sense (5' to 3')	Antisense (5' to 3')
<i>PLIN5</i>	AAGCCCTGAAGTGGGTTTC	GCATGTGGTCTATCAGCTCCA
<i>TGF-β</i>	GGCGATACCTCAGCAACCG	CTAAGGCGAAAGCCCTCAAT
<i>GAPDH</i>	CAGCCTCAAGATCATCAGCA	TGTGGTCATGAGTCCTTCCA

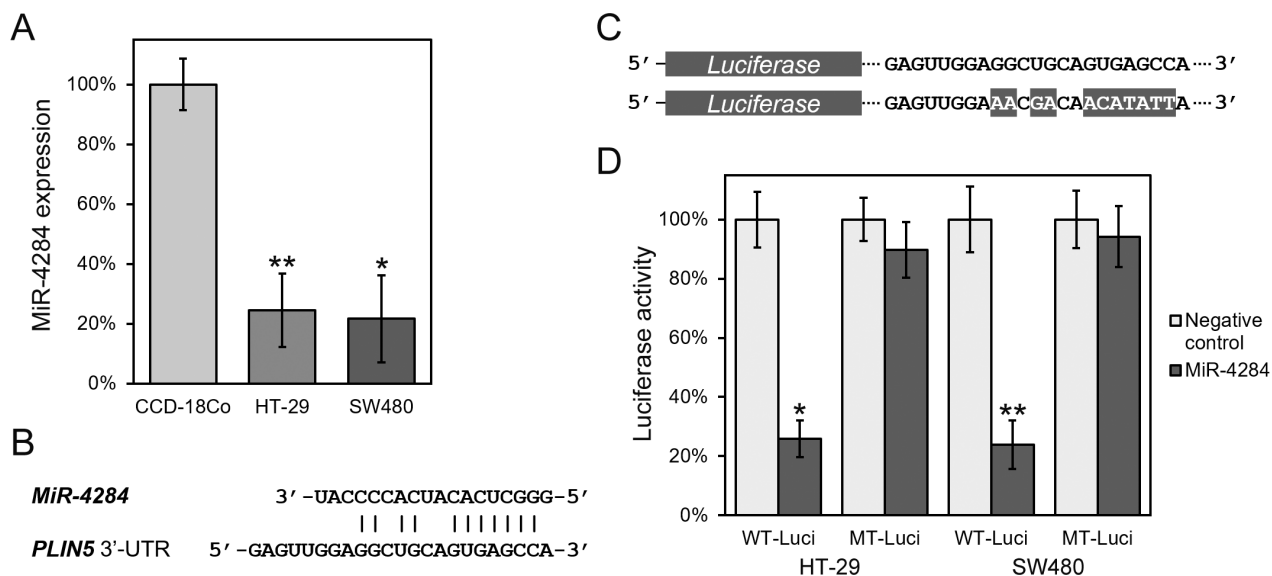


Figure 1. MiR-4284 expression is reduced in colon cancer cells, and directly targets 3'-UTR of PLIN5. (A) MiR-4284 levels in normal human colon cell line CCD-18Co compared with HT-29 and SW480 cells. (B) Sequences of putative miR-4284 binding sites on the 3'-UTR of PLIN5. (C) Schematics of luciferase reporter constructs: top, wild type (WT) luciferase construct (WT-Luci) contains original putative binding site from PLIN5 3'-UTR; bottom, mutated version (MT-Luci). (D) WT and mutated luciferase constructs along with either miR-4284 or miRNA negative control were transfected into HT-29 and SW480 cells. Luciferase activity was presented as relative to respective negative control. Values were mean \pm SD of 3 independent biological replicates; ** $P < 0.01$, * $P < 0.05$, compared to respective control.

negative control were seeded into 6-well plate post transfection. A linear cut was generated cautiously across the confluent monolayer cells with the tip of a 100 μ l sterile pipette, after which gentle washes of PBS were performed to remove the debris. Migration was quantitated as the distance the growing edge moved on the wounded monolayer after 36 h, and migration rates were calculated as the percentages relative to the appropriate control.

Cell invasion assay

Cell invasion assay was conducted using a 24-well plate with chamber inserts (pore size: 8 μ m, BD Biosciences). The hsa-miR-4284- or miRNA negative control-transfected cells (1×10^5 per well, diluted with serum-free culture medium) were fed into the upper chambers with membranes coated with Matrigel. The lower compartments received 500 μ l complete medium per well to attract cells. The cultures were maintained in the incubator at 37 $^{\circ}$ C for 24 h, and afterwards treated with 20 μ M 5-ethynyl-2'-deoxyuridine (EdU) at 37 $^{\circ}$ C for another 4 h. Membrane inserts were then detached for staining with the EdU kit (Invitrogen). For each well, six random microscopic fields were counted, and the percentage of cell numbers relative to the appropriate control was calculated as the invasion rate.

Cell attachment and detachment assay

The cells (1×10^5 cells per well) were plated in a 24-well plate. In brief, to assess cell attachment, non-attached cells were removed by two washes with PBS after incubation for 1 h, and the cells that remained attached were trypsinized

for counting. The attachment rate was calculated as the percentage of attached cells in total cells and normalized to the appropriate control. To assess detachment, cells were cultured for 24 h and then treated with 0.05% trypsin for 3 min to be detached and counted. The remaining cells still attached were further trypsinized with 0.25% trypsin for counting. The percentage of detached cells in total cells was defined as the detachment rate, normalized to the appropriate control.

Statistical analysis

All values were expressed as means \pm standard deviations (SDs). Two-tailed student's t-test was employed to examine statistical differences between treatment groups. Differences were regarded as statistically significant with p less than 0.05.

Results

MiR-4284 is down-regulated in colon cancer cell lines

First, with qRT-PCR evaluation of miR-4284 expression in human colon cancer cell lines HT-29 and SW480, we discovered that miR-4284 is markedly lower compared to its levels in the normal colon cell line CCD-18Co (Figure 1A). Next, using the TargenScanHuman webtool (16), we identified that the 3'-UTR of PLIN5 mRNA harbored a putative binding site complementary to miR-4284 (Figure 1B). These findings indicated that miR-4284, which may target PLIN5, was substantially suppressed in colon cancer cells in comparison with normal human colon cells.

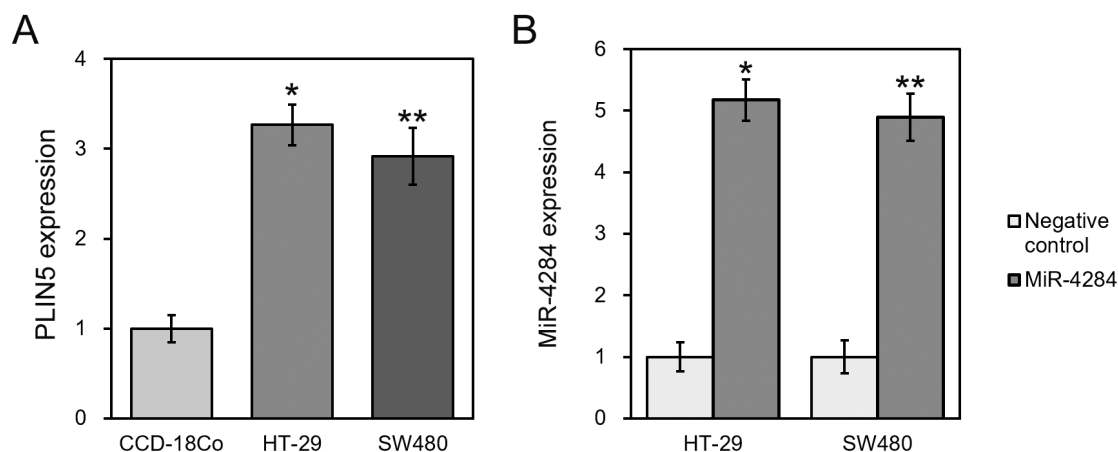


Figure 2. MiR-4284 mimic elevates miR-4284 expression in colon cancer cells. (A) PLIN5 mRNA levels in normal human colon cell line CCD-18Co compared with HT-29 and SW480 cells. (B) Relative miR-4284 levels in HT-29 and SW480 cells after transfection with either miR-4284 mimic or miRNA negative control. Values were mean \pm SD of 3 independent biological replicates; ** $P < 0.01$, * $P < 0.05$, compared to negative control.

MiR-4284 directly binds to the 3'-UTR of PLIN5

Next, we carried out validation of the putative miR-4284 binding motif on the 3'-UTR of PLIN5, employing the luciferase reporter assay. As demonstrated in **Figure 1C**, sequence from wild-type (WT-Luci) 3'-UTR of PLIN5 mRNA was constructed to the downstream of luciferase ORF, as well as its mutated version (mut-Luci). Then, these two constructs were transfected separately into both HT-29 and SW480 cells, along with miR-4284 mimic or miRNA negative control. The activity of the luciferase reporter was examined. It was consistently observed that activity of WT-Luci was dramatically reduced by miR-4284 to $\sim 30\%$ of the control, in both HT-29 and SW480 cells (**Figure 1D**). Whereas activity of mut-Luci remained mostly unaffected in miR-4284 transfected cells when compared to the control. Therefore, the complementary sequence within PLIN5 3'-UTR was

indeed directly targeted by miR-4284.

MiR-4284 inhibits PLIN5 expression in colon cancer cells

Next, we tested whether miR-4284 indeed targets PLIN5 *in vivo*. Endogenous PLIN5 mRNA level in normal human colon cell line CCD-18Co was found to be up-regulated compared with that in HT-29 and SW480 cells (**Figure 2A**). Next, both HT-29 and SW480 cells were transfected with miR-4284 as well as negative control, followed by qRT-PCR to assess the transcript level of *PLIN5*. Levels of miR-4284 in HT-29 and SW480 cells were, as expected, highly up-regulated upon transfection (**Figure 2B**). In comparison with the control, miR-4284 greatly reduced *PLIN5* mRNA levels in both lines of colon cancer cells (**Figure 3A**), evidently demonstrating that *PLIN5* was a *bona fide* target of miR-4284. With antibody against PLIN5, we verified that PLIN5 protein was drastically

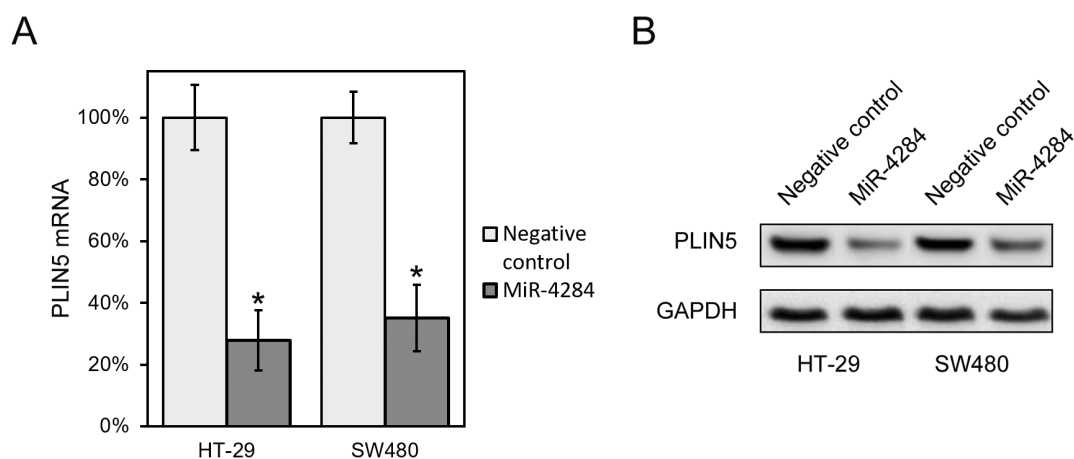


Figure 3. PLIN5 is down-regulated by miR-4284 expression in colon cancer cell lines. Levels of PLIN5 mRNA (A) and protein (B) in HT-29 and SW480 cells transfected with either miR-4284 or miRNA negative control. Values were mean \pm SD of 3 independent biological replicates; * $P < 0.05$, compared to negative control.

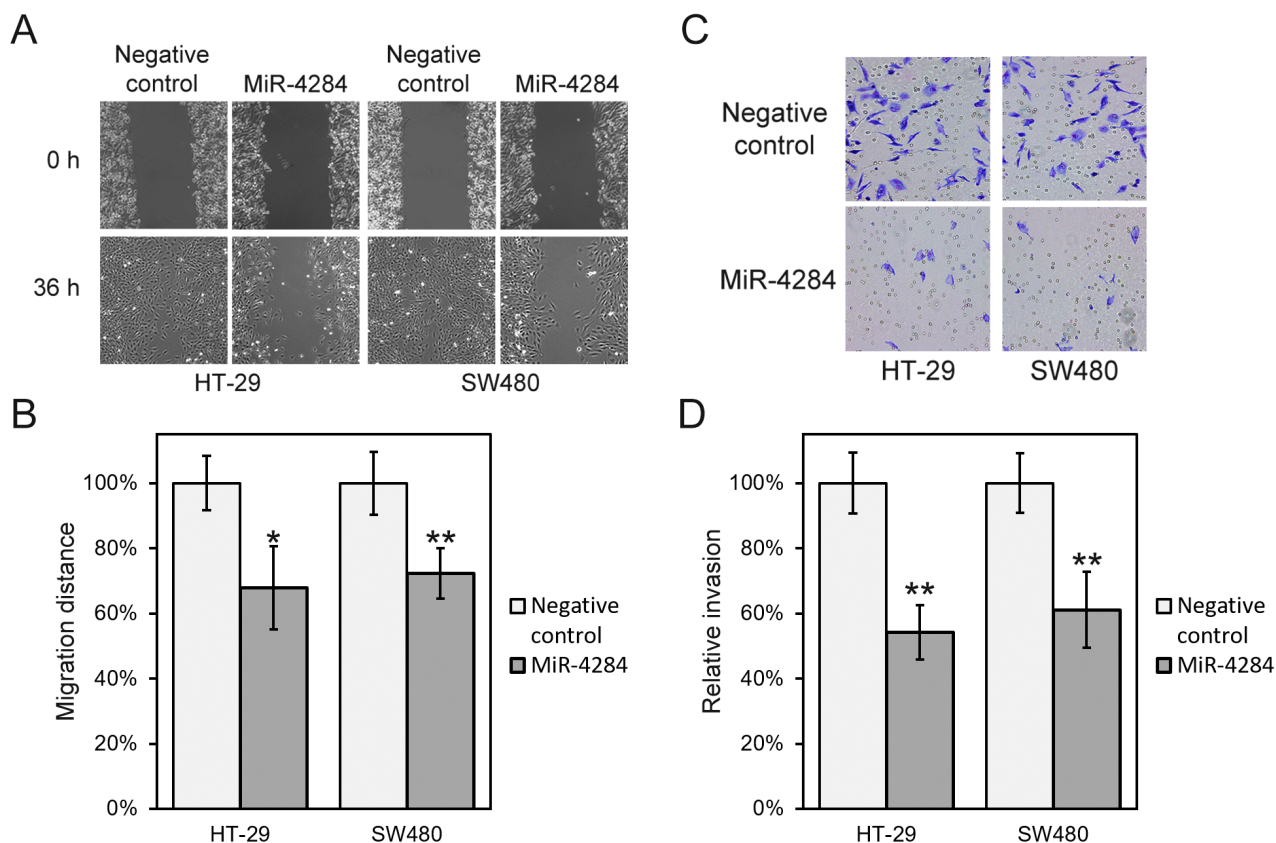


Figure 4. MiR-4284 expression suppresses migration and invasion of colon cancer cells. (A) Wound-healing assay for HT-29 and SW480 cells, transfected with either miR-4284 or negative control. (B) The migrated distances relative to respective controls at 36 h after the wound being generated were measured. (C) Cell invasion assay for HT-29 and SW480 cells, transfected with either miR-4284 or miRNA negative control. (D) The amounts of invaded cells relative to the respective control were calculated 24 h after seeding. Values were mean \pm SD of 3 independent biological replicates; ** $P < 0.01$, * $P < 0.05$, compared with negative control.

decreased as well in cells transfected with miR-4284, but not the negative control (Figure 3B).

MiR-4284 inhibits migration and invasion of colon cancer cells

In order to elucidate the role of miR-4284 in colon cancer tumorigenesis, we evaluated the wound-healing capacity and the invasive properties of miR-4284 or control miRNA transfected HT-29 and SW480 cells. Indeed, the migration rates of both cell lines were greatly reduced after miR-4284 transfection in comparison to control experiments (Figure 4A and 4B). Further, miR-4284 transfection also lowered the invasion rates of both HT-29 and SW480 cells (Figure 4C and 4D). Altogether, these data strongly indicated the anti-tumor property of miR-4284 in colon cancer.

MiR-4284 reverses the epithelial-mesenchymal transition (EMT) of colon cancer cells

As we were performing the aforementioned assays, we frequently observed morphological changes in cells when they were transfected with miR-4284. Both HT-29 and SW480 cells originally displayed an elongated fibroblastoid morphology; however, upon miR-4284 transfection both lines of cells assumed a rounded cell shape (data not shown), which suggested a loss of EMT

phenotype. To examine this possibility, we assessed attachment and detachment capacities of both lines of colon cancer cells following transfection with miR-4284 or the negative control. We found that miR-4284 dramatically lowered both attachment and detachment rates of HT-29 and SW480 cells (Figure 5A and 5B). These findings indicated an inhibition of EMT characteristics at the level of cell morphology. We further assessed if the same trend still held at the molecular level. In this context, we examined the transcript levels of E-cadherin (epithelial marker), N-cadherin and Vimentin (both mesenchymal markers). Consistently, miR-4284 reduced E-cadherin, while up-regulated N-cadherin and Vimentin, in comparison with control transfected cells (Figure 5C), suggesting reversed EMT phenotype at the protein level.

Discussion

In our current study, we showed that miR-4284 was suppressed in HT-29 and SW480 cells, both human colon cancer cell lines, with CCD-18Co cells (normal colon cell line) as the control. Interestingly, through in silico analysis, we found a putative binding site of miR-4284 on the 3'-UTR of PLIN5 mRNA. Through luciferase reporter assay, we determined that the 3'-UTR sequence was directly targeted by miR-4284. Moreover, introduction of

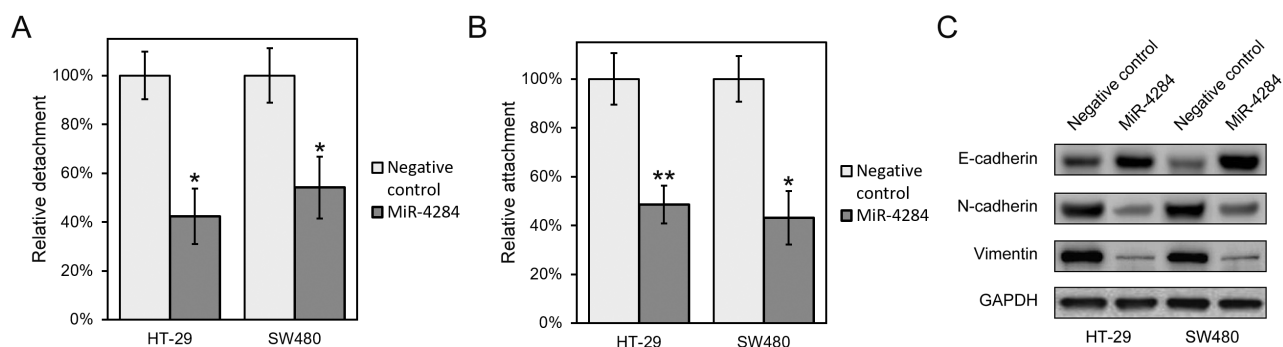


Figure 5. MiR-4284 inhibits epithelial-mesenchymal transition (EMT) of colon cancer cells. (A) Cell attachment and (B) detachment assays were conducted in HT-29 and SW480 cells transfected with either miR-4284 or miRNA negative control. Values were mean \pm SD of 3 independent biological replicates; ** $P < 0.01$, * $P < 0.05$, compared to negative control. (C) Expression of EMT phenotypic proteins was assessed in HT-29 and SW480 cells transfected with either miR-4284 or miRNA negative control.

miR-4284 into HT-29 and SW480 cells down-regulated PLIN5 at both transcript and protein levels, indicating that PLIN5 was repressed by miR-4284 *in vivo*. Further, miR-4284 expression dramatically inhibited the migratory and invasive activities of colon cancer cells, likely through reverse of EMT, as indicated by a substantial reduction in E-cadherin expression (epithelial marker) and an elevation in the expression of N-cadherin as well as Vimentin (both mesenchymal markers).

EMT refers to the vital process for differentiated epithelial cells to change status, acquiring the capacity to invade, resist apoptosis, and disseminate, which eventually leads to metastasis formation (17, 18). MiRNAs are frequently associated with the EMT of multiple human cancers, colon cancer included, by altered expression of tumor suppressor genes or oncogenes (19). For instance, in lung cancer, miR-134/487b/665 cluster affects EMT mediated by transforming growth factor- β (TGF- β) via membrane associated guanylate kinase inverted 2 (MAGI2) (20). In addition, in breast cancer miR-125b/489 reportedly regulates EMT (21, 22). Down-regulated miR-200c contributes to epidermal growth factor receptor (EGFR) inhibitor resistance through manifestation of EMT features (23). Further, miR-216a/217 was demonstrated to target SMAD7 and PTEN to induce EMT in liver cancer (24).

A recent study has identified co-regulated miRNAs with the potential to cooperate during the EMT process, by combined computational and experimental approaches (25). This study reported that miRNAs could serve as a secondary regulatory layer post transcription, enhancing transcriptional modulations on EMT-associated processes (i.e., cell-adhesion or organization of extracellular matrix) while at the same time dampening transcriptional impacts on irrelevant genes. This discovery raises significant concern over the function of miRNAs in the metastasis of cancer. In line with this recent discovery, we hereby report that a novel miR-4284 is significantly down-regulated and directly targets PLIN5 to inhibit the EMT process in colon cancer cells. Ectopic expression of miR-4284 dramatically reduced endogenous PLIN5 mRNA and protein. In addition, miR-4284 also functioned to suppress

the migration, invasion and EMT of colon cancer cells. PLIN5 belongs to the PAT (perilipin, adipophilin and TIP47) family of amphiphilic proteins, the main structural proteins associated with lipid droplet fractions (26). To date, the major function of PLIN5 is mainly to maintain lipid homeostasis by inhibiting lipolysis (27), and report on the involvement of PLIN5 in human cancer is limited. A recent investigation found that PLIN5 was robustly expressed in tumors of human patients with hepatocellular carcinoma (28). Results of our current study have brought this discovery one step further, by identifying its upstream regulator, miR-4284, whose expression directly suppresses PLIN5 in colon cancer cells. Our future study will focus on verifying the involvement of PLIN5 in colon cancer using an animal model *in vivo*.

In summary, this study presented the first data involving miR-4284 and PLIN5 in colon cancer EMT. EMT is commonly believed to correlate with the aggressiveness of cancer cells, for instance capacities to migrate and invade, hence reverse or inhibition of such transition may inspire new therapeutic strategies for cancer treatments. To this end, we discovered that miR-4284 reversed the EMT of colon cancer cell lines HT-29 and SW480, which was likely the reason miR-4284 could potentially inhibit the migratory and invasive activities of colon cancer cells. Hence, our results highlight the potential of miR-4284 as a promising target in colon cancer treatment, via inhibiting the expression of PLIN5 and EMT process of colon cancer cells.

Conflict of interest

The authors declare that they have no conflicts of interest to disclose.

Funding

This work was funded by Wuxi Taihu Lake talent project (2020THRC-GD-5); Wuxi Medical Emphasis Disciplines Funding (syxzdxx-pwk); Wuxi Science and Technology Development Plan (CZE02H1701); Top Talent Support Program for young and middle-aged people of Wuxi Health Committee (BJRC-9); Youth Science Foundation Project of Wuxi health and Health Committee (Q202048).

References

- Siegel R, Desantis C, Jemal A. Colorectal cancer statistics, 2014. *CA Cancer J Clin.* 2014;64(2):104-17.
- Arnold M, Sierra MS, Laversanne M, Soerjomataram I, Jemal A, Bray F. Global patterns and trends in colorectal cancer incidence and mortality. *Gut.* 2017;66(4):683-91.
- Guinney J, Dienstmann R, Wang X, de Reynies A, Schlicker A, Sonesson C, et al. The consensus molecular subtypes of colorectal cancer. *Nat Med.* 2015;21(11):1350-6.
- Bartel DP. MicroRNAs: genomics, biogenesis, mechanism, and function. *Cell.* 2004;116(2):281-97.
- Lee RC, Feinbaum RL, Ambros V. The *C. elegans* heterochronic gene *lin-4* encodes small RNAs with antisense complementarity to *lin-14*. *Cell.* 1993;75(5):843-54.
- Reinhart BJ, Slack FJ, Basson M, Pasquinelli AE, Bettinger JC, Rougvie AE, et al. The 21-nucleotide *let-7* RNA regulates developmental timing in *Caenorhabditis elegans*. *Nature.* 2000;403(6772):901-6.
- Pasquinelli AE, Reinhart BJ, Slack F, Martindale MQ, Kuroda MI, Maller B, et al. Conservation of the sequence and temporal expression of *let-7* heterochronic regulatory RNA. *Nature.* 2000;408(6808):86-9.
- Esteller M. Non-coding RNAs in human disease. *Nat Rev Genet.* 2011;12(12):861-74.
- Iorio MV, Croce CM. MicroRNA dysregulation in cancer: diagnostics, monitoring and therapeutics. A comprehensive review. *EMBO Mol Med.* 2012;4(3):143-59.
- Rupaimoole R, Calin GA, Lopez-Berestein G, Sood AK. miRNA deregulation in cancer cells and the tumor microenvironment. *Cancer Discov.* 2016;6(3):235-46.
- Bader AG. miR-34 - a microRNA replacement therapy is headed to the clinic. *Front Genet.* 2012;3:120.
- Li Y, Shen Z, Jiang H, Lai Z, Wang Z, Jiang K, et al. MicroRNA4284 promotes gastric cancer tumorigenicity by targeting ten-eleven translocation 1. *Mol Med Rep.* 2018;17(5):6569-75.
- Yang F, Nam S, Brown CE, Zhao R, Starr R, Ma Y, et al. A novel berbamine derivative inhibits cell viability and induces apoptosis in cancer stem-like cells of human glioblastoma, via up-regulation of miRNA-4284 and JNK/AP-1 signaling. *PLoS One.* 2014;9(4):e94443.
- Munari E, Marchionni L, Chitre A, Hayashi M, Martignoni G, Brunelli M, et al. Clear cell papillary renal cell carcinoma: micro-RNA expression profiling and comparison with clear cell renal cell carcinoma and papillary renal cell carcinoma. *Hum Pathol.* 2014;45(6):1130-8.
- McDermott N, Meunier A, Wong S, Buchete V, Maignol L. Profiling of a panel of radioresistant prostate cancer cells identifies deregulation of key miRNAs. *Clin Transl Radiat Oncol.* 2017;2:63-8.
- Agarwal V, Bell GW, Nam JW, Bartel DP. Predicting effective microRNA target sites in mammalian mRNAs. *Elife.* 2015;4.
- Gregory PA, Bert AG, Paterson EL, Barry SC, Tsykin A, Farshid G, et al. The miR-200 family and miR-205 regulate epithelial to mesenchymal transition by targeting ZEB1 and SIP1. *Nat Cell Biol.* 2008;10(5):593-601.
- Hanahan D, Weinberg RA. Hallmarks of cancer: the next generation. *Cell.* 2011;144(5):646-74.
- Wang Z, Li Y, Ahmad A, Azmi AS, Kong D, Banerjee S, et al. Targeting miRNAs involved in cancer stem cell and EMT regulation: An emerging concept in overcoming drug resistance. *Drug Resist Updat.* 2010;13(4-5):109-18.
- Kitamura K, Seike M, Okano T, Matsuda K, Miyanaga A, Mizutani H, et al. MiR-134/487b/655 cluster regulates TGF-beta-induced epithelial-mesenchymal transition and drug resistance to gefitinib by targeting MAGI2 in lung adenocarcinoma cells. *Mol Cancer Ther.* 2014;13(2):444-53.
- Jiang L, He D, Yang D, Chen Z, Pan Q, Mao A, et al. MiR-489 regulates chemoresistance in breast cancer via epithelial mesenchymal transition pathway. *FEBS Lett.* 2014;588(11):2009-15.
- Wu YM, Chen ZJ, Liu H, Wei WD, Lu LL, Yang XL, et al. Inhibition of ERRalpha suppresses epithelial mesenchymal transition of triple negative breast cancer cells by directly targeting fibronectin. *Oncotarget.* 2015.
- Shien K, Toyooka S, Yamamoto H, Soh J, Jida M, Thu KL, et al. Acquired resistance to EGFR inhibitors is associated with a manifestation of stem cell-like properties in cancer cells. *Cancer Res.* 2013;73(10):3051-61.
- Xia H, Ooi LL, Hui KM. MicroRNA-216a/217-induced epithelial-mesenchymal transition targets PTEN and SMAD7 to promote drug resistance and recurrence of liver cancer. *Hepatology.* 2013;58(2):629-41.
- Cursons J, Pillman KA, Scheer KG, Gregory PA, Foroutan M, Hedyeh-Zadeh S, et al. Combinatorial targeting by microRNAs co-ordinates post-transcriptional control of EMT. *Cell Syst.* 2018;7(1):77-91 e7.
- Kimmel AR, Brasaemle DL, McAndrews-Hill M, Sztalryd C, Londos C. Adoption of PERILIPIN as a unifying nomenclature for the mammalian PAT-family of intracellular lipid storage droplet proteins. *J Lipid Res.* 2010;51(3):468-71.
- Yamaguchi T, Matsushita S, Motojima K, Hirose F, Osumi T. MLDP, a novel PAT family protein localized to lipid droplets and enriched in the heart, is regulated by peroxisome proliferator-activated receptor alpha. *J Biol Chem.* 2006;281(20):14232-40.
- Asimakopoulou A, Vucur M, Luedde T, Schneiders S, Kalampoka S, Weiss TS, et al. Perilipin 5 and lipocalin 2 expression in hepatocellular carcinoma. *Cancers (Basel).* 2019;11(3).

Nerol protects against hypoxia/reoxygenation-induced apoptotic injury by activating PI3K/AKT signaling in cardiomyocytes

Jin CHENG, Qing ZOU, Yugang XUE*

Department of Cardiology, Tangdu Hospital, Air force Military Medical University, Xi'an 710000, China.

*Correspondence: xueyugang123456@163.com
<https://doi.org/10.37175/stemedicine.v2i6.87>

ABSTRACT

Background: Nerol was reported as a natural anti-oxidant product and its protective effects against cardiovascular diseases have been documented. Our current study was designed to explore the cardioprotective effect of Nerol on hypoxia/reoxygenation (H/R)-induced production of reactive oxygen species (ROS) and cell apoptosis in H9c2 cells. The potential molecular mechanisms were further investigated.

Methods: The cells were treated with 2.5 or 5 μ M Nerol before or after H/R. Lactate dehydrogenase (LDH) release, cell viability, oxidative stress markers, and apoptotic proteins were assessed by cell counting kit-8, LDH release assay, commercial kits, and Western blot, respectively. To explore the underlying mechanism, the phosphorylation of p85 and p38, regulatory subunits of phosphoinositide-3-kinase (PI3K)/protein kinase B (AKT) and mitogen-activated protein kinase (MAPK), was evaluated by Western blot. To further confirm that the PI3K/AKT signaling pathway participated in the cardiomyocyte protection, H9c2 cells were treated with 5 μ M Nerol in the presence or absence of 5 μ M BEZ235 or LY294002 followed by H/R treatment.

Results: H/R remarkably induced apoptosis, LDH release and ROS production. The cell viability was suppressed via inhibiting the PI3K/AKT signaling pathway activation. By contrast, pretreatment with Nerol can neutralize these effects by activating the PI3K/AKT signaling pathway. With the addition of BEZ235 or LY294002, the inhibitory effects of Nerol were abolished.

Conclusion: Nerol provided promising cardioprotective effect against H/R-induced injuries in H9c2 cells by activating the PI3K/AKT pathway.

Keywords: Nerol · Oxidative stress · Hypoxia/reoxygenation · Apoptosis · PI3K/AKT signaling

Introduction

The heart is a high oxygen consumption organ and the cardiomyocytes are very sensitive to oxygen deprivation (1). The reoxygenation following hypoxia normally causes massive production of reactive oxygen species (ROS), which results in oxidative damage in the pathophysiology of hypoxia/reoxygenation (H/R) injury (2). Overwhelming ROS production results in remarkable damage to

cardiomyocytes and impairs the balance between oxidation and antioxidation (3). Oxidative stress is one of the main contributions to apoptosis, thus alleviating and inhibiting ROS production may be a potential therapeutic approach to promote survival and inhibit apoptosis of cardiomyocytes (4).

Discovering and developing a novel natural product to prevent and treat cardiovascular diseases resulted from oxidative stress is very meaningful (5-7). The cardioprotective effects of grape seed proanthocyanidin extract against cardiomyocyte apoptosis, DNA damages and histopathological changes have been attributed to its superior antioxidant efficacy (6). Quercetin, a flavonoid anti-oxidant present in vegetables and fruits, also shows

Received: Mar 12, 2021; Accepted: Mar 25, 2021.

© The Author(s). 2020 This is an **Open Access** article distributed under the terms of the Creative Commons License (<http://creativecommons.org/licenses/by/4.0/>) which permits unrestricted use, distribution, and reproduction in any medium or format, provided the original work is properly cited.

cardioprotective effects through its anti-oxidative stress property (7). Previous study has revealed the cardioprotective effects of Rosa Damascene petals against myocardial infarction in rats by restoring the cardiac marker enzymes and increasing myocardial anti-oxidants (8). Nerol, one of the main chemical compositions in Rosa damascene, is known as a common constituent of several essential oils (9). It has been demonstrated that Nerol in the essential oils promotes the superoxide scavenging activities (10). The anti-oxidant potential of Nerol attracts widespread interest (9). Nerol shows a promising anti-oxidant property in hydroperoxide-stressed rat alveolar macrophages, which promotes cell viability and inhibits ROS generation (11). After being pretreated with Nerol, the arrhythmia severity index can be significantly attenuated by reducing Ca^{2+} influx in guinea pig hearts (12). However, it is largely unknown concerning the cardioprotective effects of Nerol against H/R-induced injuries in cardiomyocytes.

Materials and Methods

Cell culture and treatment

H9c2 cells (a rat embryonic heart cardiomyocyte cell line) was acquired from the American Type Culture Collection (ATCC, Manassas, VA). The cells were cultured in Dulbecco's modified Eagle's medium (DMEM, Invitrogen), 10% fetal bovine serum (FBS, Gibco), and 1% penicillin/streptomycin (1%) at 37 °C in a humidified culture incubator (5% CO_2 and 95% air).

H/R model

To evaluate the H/R-induced injury, H9c2 cells with or without Nerol treatment were cultured in serum- and glucose-free medium and incubated under hypoxic conditions (94% N_2 , 1% O_2 and 5% CO_2) for 12 h at 37 °C, and then cultured under reoxygenation conditions (5% CO_2 and 95% air) in complete medium for another 12 h at 37 °C. The cells cultured under normoxic conditions were used as the control group. To determine the effects of Nerol on H/R-induced injuries, H9c2 cells were pretreated with 2.5 or 5 μM Nerol (Figure 1A, Selleckchem, Houston, TX), followed by hypoxia (12 h) and reoxygenation (12 h). To determine the potential therapeutic role of Nerol in pathological cardiac patients, the H9c2 cells were treated with Nerol after hypoxia/reoxygenation-induced injury. The corresponding lactate dehydrogenase (LDH) release and cell viability were determined. To evaluate the effects of Nerol on H9c2 cells following the treatment of phosphoinositide-3-kinase (PI3K) inhibitors, H9c2 cells were incubated with the serum- and glucose-free medium supplemented with Nerol (5 μM) with or without BEZ235 (5 μM , a

dual PI3K/mTOR inhibitor, Sigma) or LY294002 (a strong PI3K inhibitor, Sigma), before H/R induction as aforementioned.

Cell viability determination

Cell counting kit-8 (CCK-8) assay was used to evaluate cell viability. Briefly, H9c2 cells were seeded to 96-well plates with 5×10^4 cells per well and treated with Nerol, followed by incubating with the CCK-8 reagent at 37 °C with 5% CO_2 for another 2 h. A microplate reader was used to read the absorbance at a wavelength of 450 nm.

LDH release assay

The LDH level was determined to evaluate the H/R-induced cell necrosis according to the manufacture's instruction (Takara, Dalian, China). The cells were subjected distinct treatments as mentioned before. The supernatant was carefully collected after the microplate was centrifuged at 250 g for 10 min. The supernatants were incubated with the reaction mixture for 30 min at room temperature. A microplate reader was used to read the absorbance at a wavelength of 490 nm.

Oxidative stress marker analysis

The levels of glutathione peroxidase (GSP-Px), catalase (CAT), superoxide dismutase (SOD) and malondialdehyde (MDA) were measured by commercial assay kits (Beyotime, Shanghai, China). In brief, the cells were lysed and homogenized by 1% Nonidet P-40 (NP-40, Sigma-Aldrich) lysis buffer containing 20 mM Tris, 137 mM NaCl, 20% glycerol, 10 mM NaF, 1 mM Na_3VO_4 , 10 mM phenylmethylsulfonyl fluoride, and 1 \times proteinase inhibitor cocktail, pH 7.4. The activity of CAT, GSH-Px and MDA in the homogenates was determined. To determine the activity of SOD, the cells were washed by ice-cold phosphate-buffered saline (PBS) and lysed by provided lysis buffer. The homogenate was centrifuged at 12,000 g for 5 min at 4 °C. The supernatant was collected to determine the concentration of SOD.

Cell apoptosis analysis

A commercial Annexin V-FITC/propidium iodide (PI) apoptosis detection kit (Sigma-Aldrich) was used to analyze the H9c2 cells with different treatments as described above. The cells were trypsinized and washed with cold PBS, followed by resuspending in 1 \times binding buffer. H9c2 cells were further incubated with PI and FITC Annexin V for 13-15 min in the dark. The apoptotic cells were quantified by flow cytometry using a FACScan flow cytometry and CellQuestTM software (BD Biosciences, San Jose, CA, US).

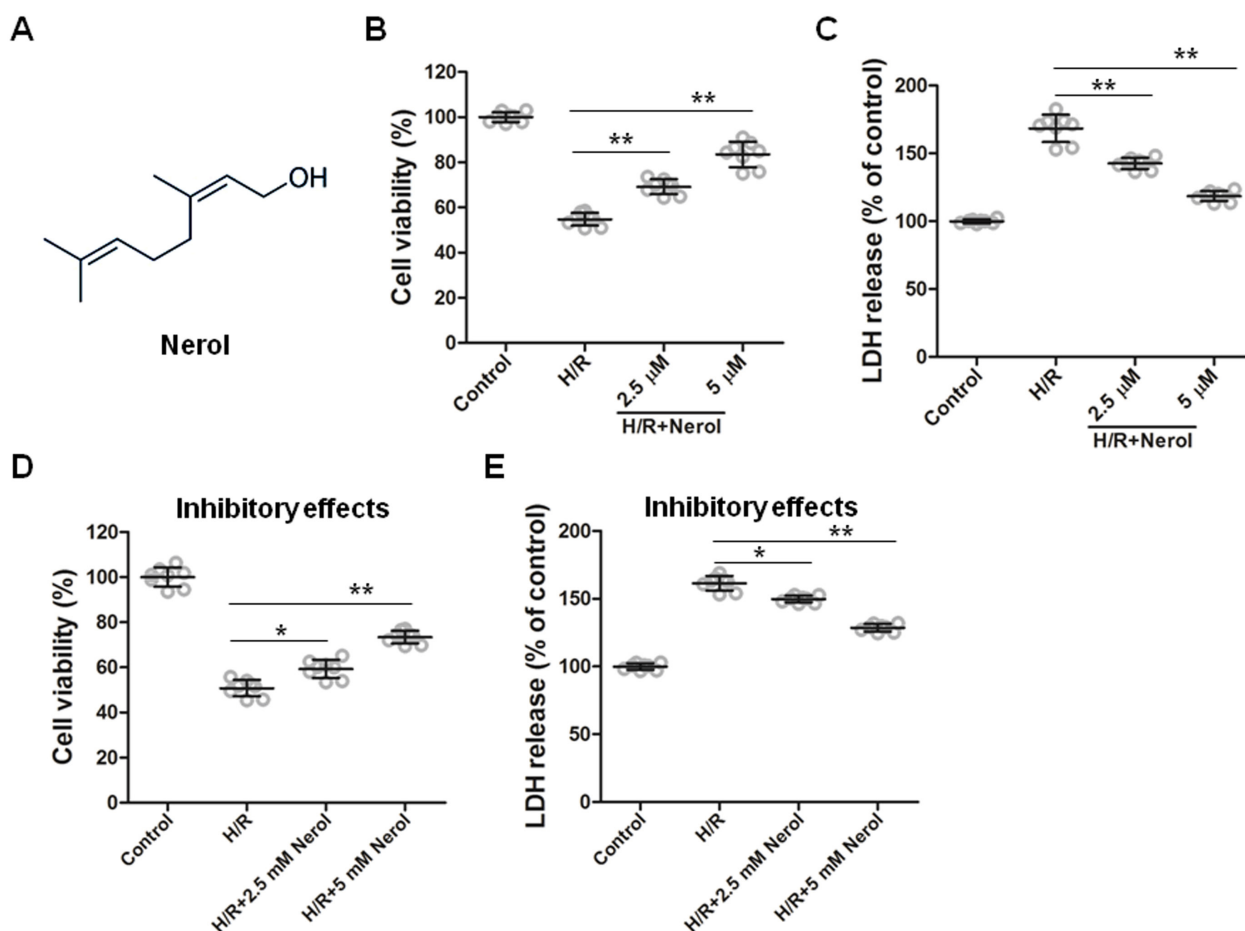


Figure 1. Nerol alleviated H/R-induced injuries in cardiomyocytes. (A) Chemical structure of Nerol. (B) H9c2 cardiomyocytes were treated with 2.5 μ M or 5 μ M Nerol, followed by H/R treatment for 12/12 h, followed by CCK-8 assay. (C) H9c2 cardiomyocytes were treated with 2.5 μ M or 5 μ M Nerol, followed by H/R treatment for 12/12 h, followed by LDH release assay. (D) H9c2 cardiomyocytes were pre-treated with H/R treatment for 12 h, followed by 2.5 μ M or 5 μ M Nerol for 12 h, followed by CCK-8 assay. E. H9c2 cardiomyocytes were pre-treated with H/R treatment for 12 h, followed by 2.5 μ M or 5 μ M Nerol for 12 h, followed by LDH release assay. n=8. $p < 0.05$ (*), $p < 0.01$ (**).

Western blot analysis

The total protein concentrations in the whole cell lysate were measured by using the Bicinchoninic Acid (BCA) Protein Assay Kit (Thermo Scientific, Rockford, IL) and 20-30 μ g protein aliquots were denatured by heating at 95°C for 10 min in sodium dodecyl sulfate (SDS) loading buffer. Protein was separated on a 12% SDS-polyacrylamide gel electrophoresis (PAGE) gel and then transferred to polyvinylidene difluoride membranes. The following primary antibody were used: poly (ADP-ribose) polymerase (PARP); cleaved PARP; MCL-1; Bim; phosphor-p85 (p-p85); PI3K p85; phosphor-AKT (p-AKT); total-AKT; phosphor-p38 (p-p38); mitogen-activated protein kinase (MAPK) p38; and glyceraldehyde 3-phosphate dehydrogenase (GAPDH). Antibodies were provided by Cell Signaling. The relative protein expression levels were normalized to GAPDH by ImageJ software.

Caspase-3 activity assay

To evaluate the activity of caspase-3 in H9c2 cells with different treatments, a colorimetric caspase-3

activity assay kit (Beyotime) was used according to the manufacture's instruction. A microplate reader was used to read the absorbance at a wavelength of 485 nm.

Statistical analysis

The data were presented as mean \pm standard deviation (SD), which was confirmed by at least three independent experiments. One-way analysis of variance (ANOVA) models with Tukey's post-hoc tests were used. P value less than 0.05 was considered statistically significant.

Results

Nerol ameliorated H/R-induced injury in H9c2 cells in a dose-dependent manner

Comparing to the cells cultured in normoxic conditions, H2c9 cells had significantly lower cell viability and higher LDH release after H/R induction (Figure 1B & C). In contrast, the cell viability was promoted while LDH release was inhibited by the treatment with Nerol, respectively (Figure 1B & C). Additionally, the cell

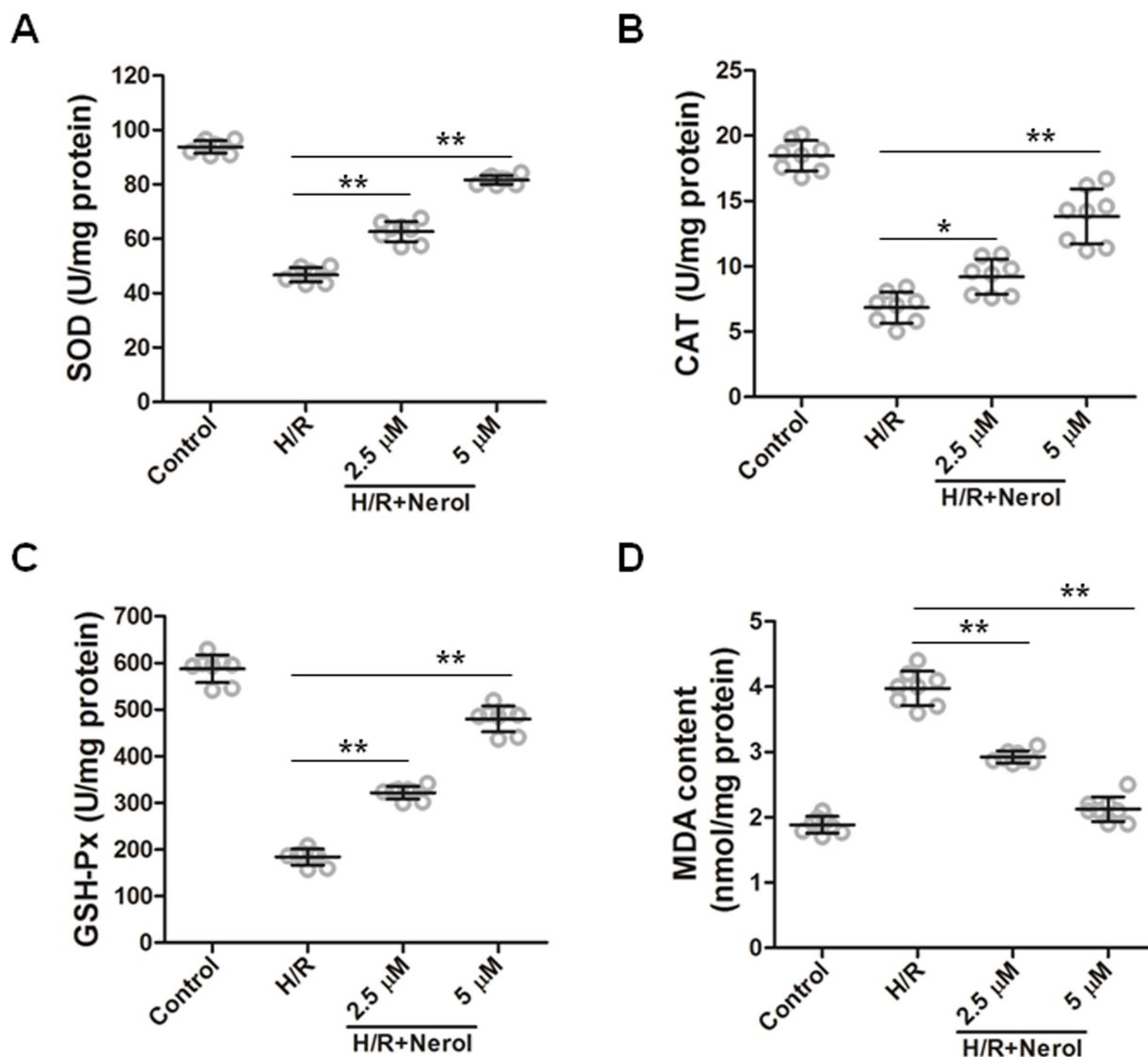


Figure 2. Nerol suppresses H/R-induced oxidative stress in cardiomyocytes. H9c2 cardiomyocytes were treated with 2.5 μM or 5 μM Nerol, followed by H/R treatment for 12/12 h. The activities of SOD (A), CAT (B), GSH-Px (C) and MDA content (D) were measured in H9c2 cardiomyocytes. $n=8$. $p<0.05$ (*), $p<0.01$ (**).

viability increased and LDH release decreased with increasing Nerol concentration (**Figure 1B & C**), indicating the effects of Nerol on cell viability and LDH release exhibited a dose-dependent manner. The above results showed that Nerol displayed protective effects against H/R injury. Moreover, we also examined the inhibitory effects of Nerol by treating the cells after H/R-induced injury, and found that cell viability and LDH release were significantly promoted and inhibited, respectively (**Figure 1D & E**). These results revealed the protective and inhibitory effects of Nerol against pre- and post-H/R-induced injuries, respectively.

Nerol ameliorated H/R-induced oxidative stress injury in H9c2 cells in a dose-dependent manner

To investigate the effect of Nerol on H/R induced oxidative in H9c2 cells, the activities of oxidative stress markers were measured. The levels of SOD, CAT and

GSH-Px were markedly decreased compared to the cells cultured under normoxic conditions; however, the levels of these markers in the cells with Nerol treatments were notably higher than the H/R stimulation (**Figure 2A, B, & C**). With Nerol concentration increased, the activities of Nerol on the anti-oxidant enzyme also increased. Interestingly, H/R stimulation remarkably promoted MDA content, which could be inhibited by the application of Nerol regardless of concentrations (**Figure 2D**). The effect of Nerol on MDA production also exhibited a dose-dependent manner and MDA content decreased with increasing Nerol concentration (**Figure 2D**).

Nerol inhibited cell apoptosis in a dose-dependent manner

To evaluate the effects of Nerol on H9c2 cell apoptosis after processed H/R treatment, flow cytometry analysis was used. Compared to the control, the H/R-treated cells showed a significantly higher apoptotic rate; however,

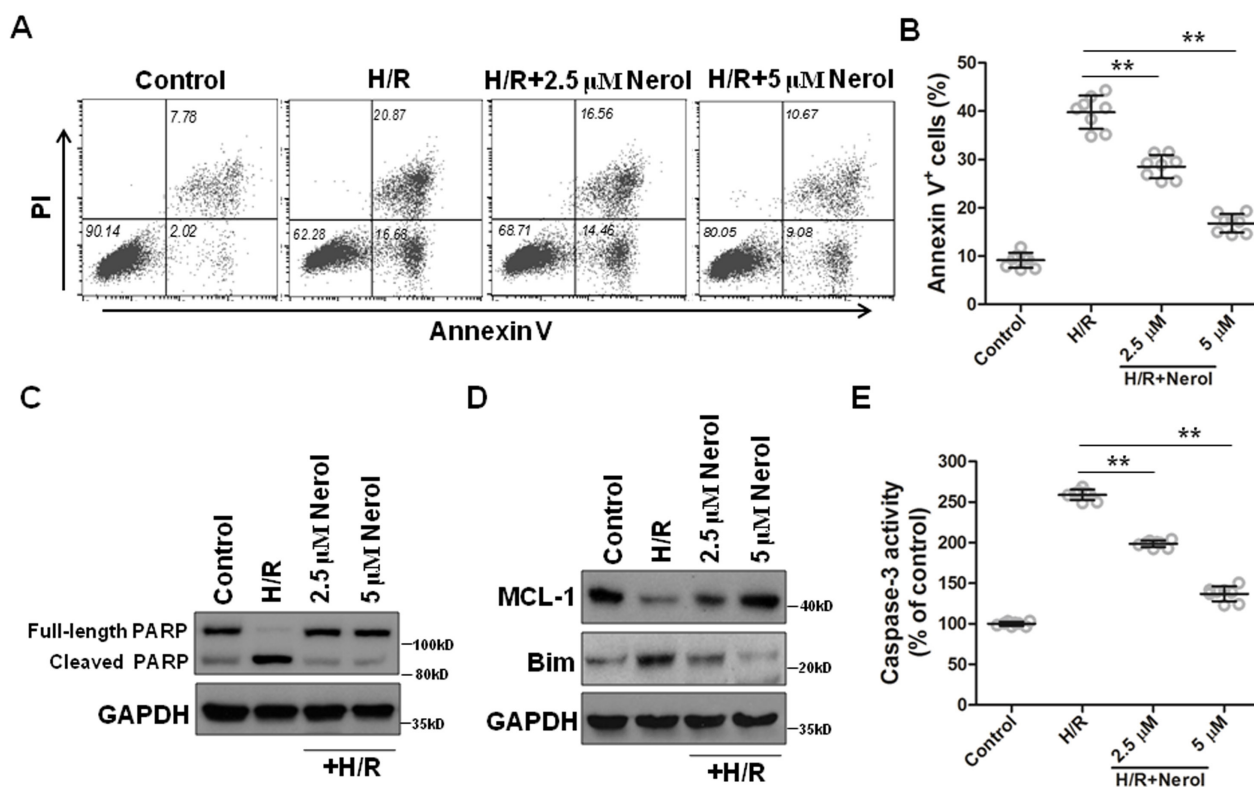


Figure 3. Nerol inhibited H/R-induced apoptosis in cardiomyocytes. (A & B) H9c2 cardiomyocytes were treated with 2.5 μM or 5 μM Nerol, followed by H/R treatment for 12/12 h. And then cells were stained with Annexin V-FITC and PI, followed by cell apoptosis analysis on a flow cytometer (A). Percentages of annexin V+ are indicated (B). (C) H9c2 cardiomyocytes were treated with 2.5 μM or 5 μM Nerol, followed by H/R treatment for 12/12 h. Then, cells were lysed for western blot against PARP, a biomarker of cell apoptosis. (D) The above cells were also lysed for western blot against MCL-1 and Bim. GAPDH was used as a loading control. E. The activity of caspase-3 in treated H9c2 cardiomyocytes was examined by caspase-3 activity assays. n=8. p<0.01 (**).

Nerol decreased apoptotic rate regardless of its concentrations (Figure 3A & B). Meanwhile, the expression of cleaved PARP and Bim was enhanced due to H/R induction; while the expression of full-length PARP and MCL-1 was abolished (Figure 3C & D). By contrast, the application of Nerol significantly suppressed the protein levels of cleaved PARP and Bim, and promoted the expression of full-length PARP and MCL-1 in a dose-dependent manner (Figure 3C & D), suggesting Nerol alleviated the H/R-induced apoptotic protein expression and inhibited the cleavage of PARP. To further confirm the inhibitory effect of Nerol on H/R-induced apoptosis in H9c2 cells, the activity of caspase-3 was quantified. The results showed that the H/R stimulation significantly promoted the caspase-3 activity, which could be suppressed by Nerol (Figure 3E). Collectively, with the Nerol concentration increased, the cell apoptosis rate, the apoptotic protein expression (cleaved PARP and Bim), and the caspase-3 activity also decreased. These results indicated that Nerol ameliorated H/R-induced cell apoptosis in H9c2 cells in a dose-dependent manner.

Nerol upregulated PI3k/AKT and MAPK signaling pathways in H9c2 cells

Compared to the control cells, H/R stimulation

significantly inhibited PI3K p85, AKT and MAPK p38 phosphorylation (Figure 4A-F). As shown in Figure 4, the phosphorylation of PI3K p85, AKT and MAPK p38 was remarkably upregulated in response to Nerol treatment regardless of the concentrations. These above results indicated that Nerol upregulated PI3K/AKT and MAPK signaling pathways in H/R-stimulated H9c2 cells.

Nerol inhibited H/R-induced injury by activation of PI3K in H9c2 cells

To evaluate whether the cardioprotective effects of Nerol on H9c2 cells were mediated via the PI3K/AKT signaling pathway, the cell viability and LDH release were measured after treatment of PI3K inhibitors (BEZ235 or LY294002). There was no significant differences between the cells treated with Nerol and the control in terms of cell viability and LDH release (Figure 5). In contrast, the cells treated with both Nerol and BEZ235 displayed significantly lower cell viability and greater LDH release after H/R stimulation than the cells treated with Nerol alone (Figure 5A & B). Besides, the cell viability and LDH release in cells treated with both Nerol and LY294002 were also restored (Figure 5C & D). Collectively, these results indicated that Nerol alleviated H/R-induced injury through activating PI3K in H9c2 cells.

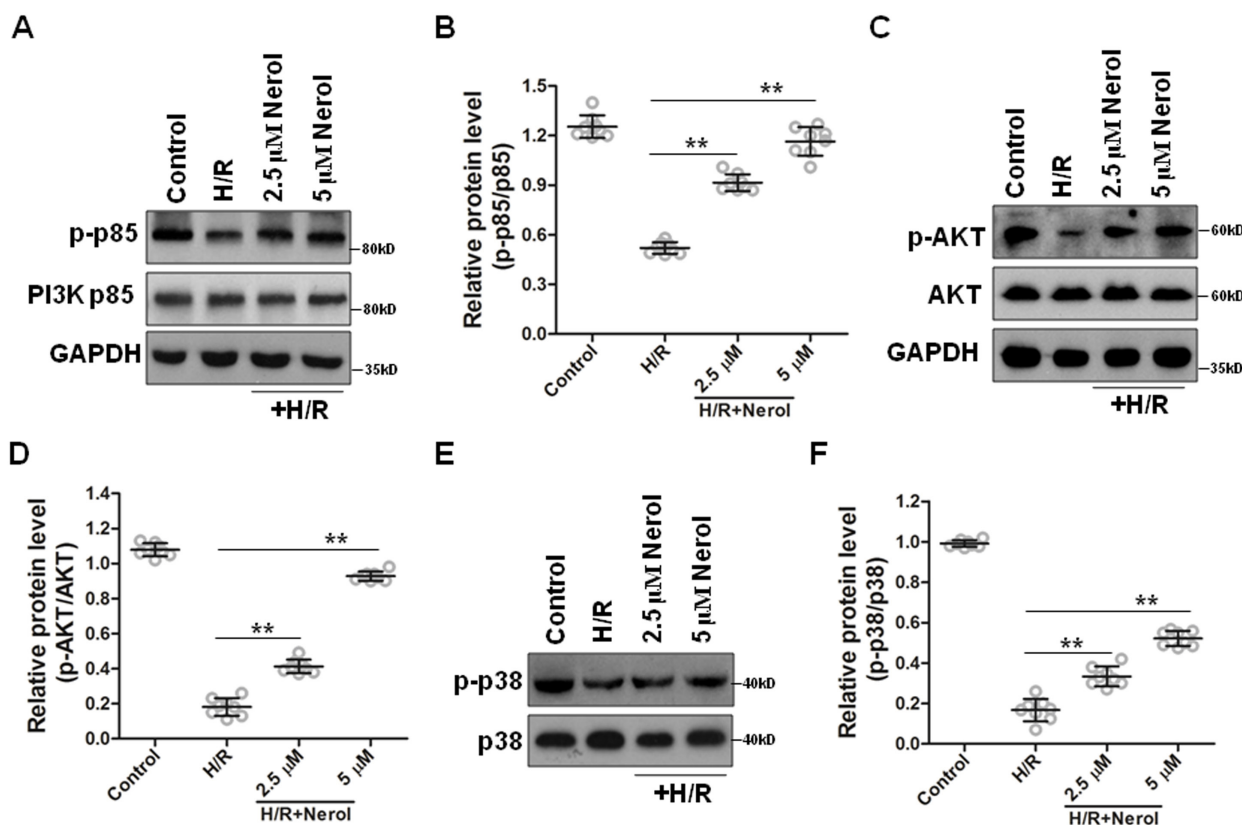


Figure 4. Nerol upregulated PI3K/AKT signaling and MAPK signaling in cardiomyocytes. (A & B) H9c2 cardiomyocytes were treated with 2.5 μ M or 5 μ M Nerol, followed by H/R treatment for 12/12 h. Then, cells were lysed for western blot against p-p85 and p85 (A). Optical density analysis for p-p85 was indicated (B). (C & D) H9c2 cardiomyocytes were treated with 2.5 μ M or 5 μ M Nerol, followed by H/R treatment for 12/12 h. Then, cells were lysed for western blot against p-AKT and AKT (C). Optical density analysis for p-AKT was indicated (D). (E & F) H9c2 cardiomyocytes were treated with 2.5 μ M or 5 μ M Nerol, followed by H/R treatment for 12/12 h. Then, cells were lysed for western blot against p-p38 and p38 (E). Optical density analysis for p-p38 was indicated (F). n=8. **p<0.01 (**).

Discussion

This study indicated that Nerol protected cardiomyocytes against H/R-induced injuries, during which the PI3K/AKT signaling pathway might be involved. This was evidenced by increased cell viability, oxidative stress marker activities (SOD, CAT, and GSH-Px) and Bcl-2 family protein expression. Moreover, the decreased LDH release, the expression of cell-death proteases, and the increased caspase-3 activity also confirmed our findings. Finally, we found that the inhibiting PI3K/AKT activation diminished the protective effects of Nerol.

The *in vitro* H/R model has been widely used to mimic several cardiac pathological situations, and it is easy to control the physical and chemical environment in the H/R model (13). Mounting evidence demonstrates that H/R is sufficient to cause injuries in various cell types through *in vitro* experiments. Thus, cellular models of H/R are useful tools to evaluate the potent cardiac protective effects of novel agents (14). Both necrosis and apoptosis are associated with the microenvironment homeostasis disrupted by cellular hypoxia and linked to excess intracellular ROS production (14, 15). Herein, we revealed that cell viability was inhibited, LDH release was elevated, oxidative stress markers were upregulated, and caspase-3 activity was enhanced upon H/R stimulation

in H9c2 cells, suggesting that H/R can indeed induce myocardial injury *in vitro*.

Nerol, an acyclic monoterpene alcohol, has been studied as an anti-oxidant and free radical scavenger (9). Previous studies reveal that Nerol significantly promoted cell viability, SOD activity and glutathione content in pre-oxide stressed rat alveolar macrophages; meanwhile, the lipid peroxidation, nitrogen oxide release and ROS generation were suppressed (11). To confirm the inhibitory effects of Nerol on cell apoptosis and necrosis, the expression of hallmark apoptotic and necrotic proteins was analyzed in our present study. The activity of caspases 3 cleaves PARP in fragments of 89 and 24 kDa during apoptosis (16). The function of full-length PARP is to repair DNA damage in response to a variety of cellular stresses via adding poly (ADP ribose) polymers (17). Moreover, caspase-3 is considered as one of the executor caspases in apoptosis and initiates apoptotic DNA fragmentation (18). In our current study, the activities of caspase 3 and cleaved PARP were enhanced, indicating cell apoptosis upon H/R stimulation. In contrast, the expression of cleaved PARP and the caspase 3 activity were restored in the Nerol-pretreated cells, indicating that Nerol may play an important role in protecting DNA against the oxidative stress-induced damage. The effects

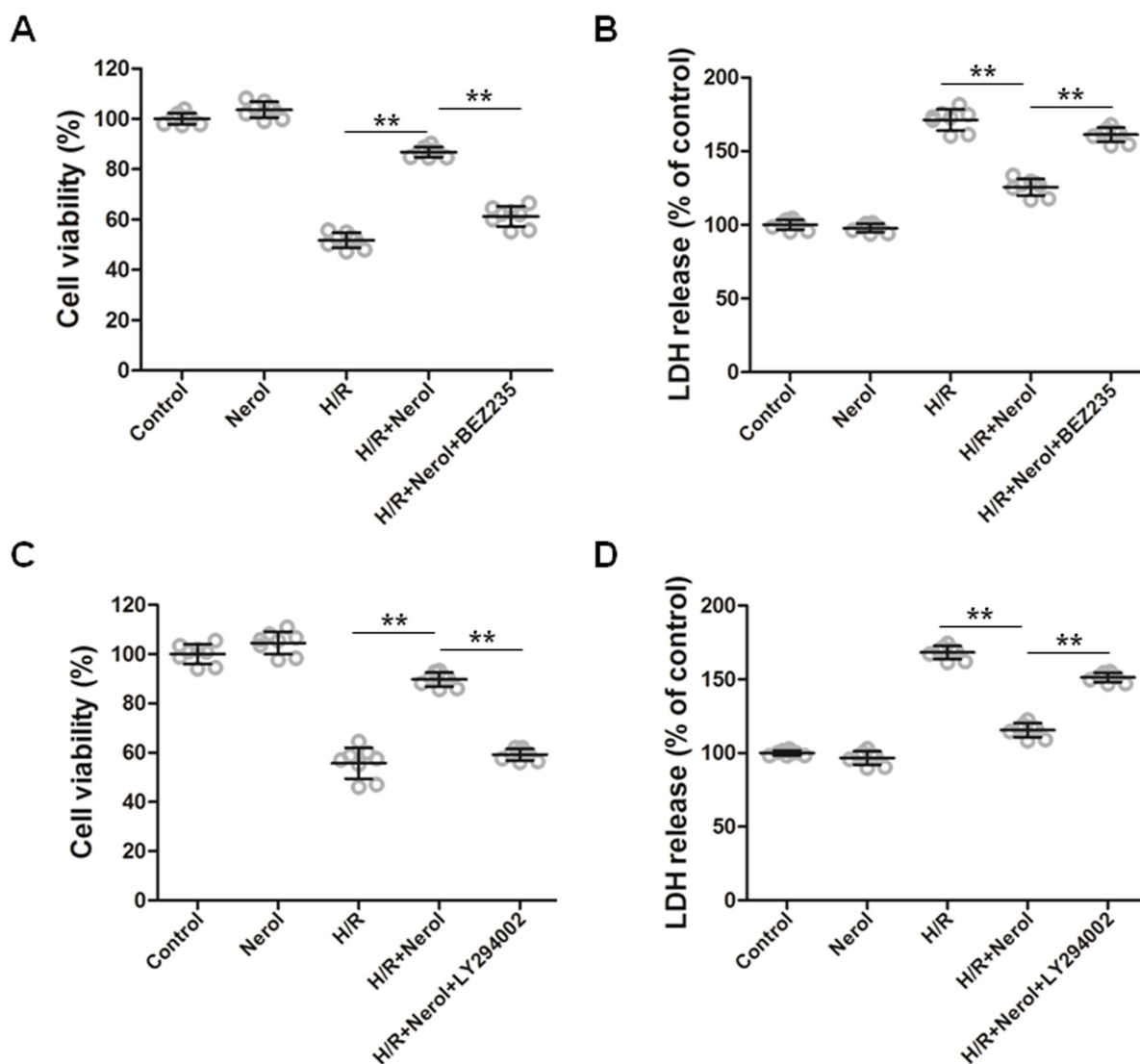


Figure 5. The effects of Nerol were abolished by the addition of PI3K inhibitors in cardiomyocytes. (A & B) H9c2 cardiomyocytes were treated with 5 μ M Nerol in the presence or absence of 5 μ M BEZ235, followed by H/R treatment for 12/12 h, or H9c2 cardiomyocytes were only treated with 5 μ M Nerol for 24 h. Then, cell viability was evaluated by CCK-8 assay (A), and LDH release was estimated by LDH release assay (B). (C & D) H9c2 cardiomyocytes were treated with 5 μ M Nerol in the presence or absence of 5 μ M LY294002, followed by H/R treatment for 12/12 h, or H9c2 cardiomyocytes were only treated with 5 μ M Nerol for 24 h. Then, cell viability was evaluated by CCK-8 assay (C), and LDH release was estimated by LDH release assay (D). n=8. p<0.01 (**).

of Nerol on the expression of MCL-1, an anti-apoptotic Bcl-2 family protein, confirmed these findings. In a cardiomyocyte-specific MCL-1 knockout mouse model, the progression of heart failure was delayed and the survival was extended (19). Silencing Bim was also shown to significantly attenuate oxygen deprivation-induced apoptosis in H9c2 cardiomyocytes (20). The expression of Bim in the H9c2 cells with Nerol pretreatment was diminished, suggesting that Nerol may inhibit cell apoptosis via negatively regulating Bim degradation. The findings of our study are consistent with these earlier reports and may suggest that the pretreatment with Nerol can significantly protect cardiomyocytes from H/R-induced apoptosis via mediating apoptotic protein expression.

To explore the potential mechanisms underlying Nerol mediated H9c2 cell apoptosis, the PI3K/AKT and

MAPK signaling pathways were evaluated. In various cell systems, activation of PI3K/AKT stimulates cell proliferation, growth and survival. In the heart, due to the limited proliferative capacity, this pathway plays a critical role in regulating cardiomyocyte growth and survival (21, 22). PI3K is composed of a catalytic subunit p110 and a regulatory subunit p85. Increasing evidence has demonstrated that p85 can mediate PI3K signal down-regulation via binding to 3-poly-PtdIns or Scr homology region 2 domain-containing phosphatase-1 (SHP-1) phosphatase (23). AKT is the key downstream effector of PI3K in regulating cardiac growth (21). In our current study, we found that after exposed to Nerol, the phosphorylation of AKT and p85 was significantly promoted, indicating that the upregulated phosphorylation of AKT and p85 is associated with cell apoptosis and

viability. In numerous systems, the activation of PI3K/AKT can provide pro-survival signals to prevent cell apoptosis. Constitutively activating PI3K or AKT can reduce hypoxia-induced apoptosis *in vitro* and cause remarkably reduced cardiomyocyte apoptosis and infarct size *in vivo* (24). Moreover, the cardiac function and morphology can be preserved both *in vitro* and *in vivo* as a result of AKT activation (22). Taken together, our findings suggested that the application of Nerol might be beneficial in cardiomyocytes *in vitro* through activating the PI3K/AKT signaling pathway. Interestingly, we also found that the phosphorylation of MAPK p38 was enhanced following Nerol pretreatment compared to the H/R control without pretreatment, indicating that the MAPK signaling pathway may also be involved. However, the detailed interaction between Nerol and the MAPK signaling pathway and the potential mechanisms are still elusive. In our further investigation, the effects of Nerol on the MAPK signaling will be studied.

To confirm the role of PI3K/AKT signaling pathway on the Nerol-mediated cardiac protection, BEZ235 and LY294002, two specific PI3K inhibitors, were used in the current study. The enhanced cell viability and LDH release in the Nerol pretreated cells were abolished following the addition of BEZ235 or LY294002. The PI3K/AKT/mTOR signaling cascade plays a critical role in cell proliferation, survival and metabolism. The core components of the PI3K/AKT/mTOR cascade are composed of PI3K and its downstream mediators AKT and mTOR (25). BEZ235 is a dual PI3K/mTOR inhibitor and inhibits both PI3K and mTOR kinase activities via binding to the adenosine triphosphate (ATP)-binding sites of PI3K and mTOR (26). Additionally, BEZ235 can inhibit several downstream effectors, such as AKT, ribosomal protein S6 and translation initiation factor 4E binding protein 1 (27). To explore the target signaling pathway, LY294002, a reversible inhibitor of PI3K and mTOR, was used to treat H9c2 cells. Similarly, the elevated cell viability and LDH release from the pretreatment of Nerol was abolished, further confirming that Nerol ameliorated the H/R-induced injuries via activating the PI3K/AKT signaling pathway. However, some limitations existed in the current study. Firstly, previous studies revealed that distinct potassium channels protected cardiac injuries via interacting with the PI3K/AKT signaling pathway (22, 28). The genetic loss of tandem pore domain acid sensitive K⁺ (TASK-1) channel can preserve cardiac function in a pressure overload model, which is associated with the AKT phosphorylation augmentation (22). Our current study demonstrated that both PI3K/AKT and MAPK signaling pathways were involved in the protective effects of Nerol on cardiomyocytes. Additionally, selectively inhibiting the PI3K signaling pathway can reverse the alleviating effects of Nerol; however, the detailed molecular mechanisms are elusive. Furthermore, the impact of Nerol on the MAPK signaling pathway is elusive. Therefore, in our further investigation, it is necessary to determine the potential direct targets of Nerol. Secondly, H9c2 cells were employed in the present study, and the *in vitro*

protective effects were revealed; thus, the potential *in vivo* cardio-protective effects of Nerol are warranted in further investigation. Thirdly, the H9c2 cell line is a rat embryonic cardiomyocyte cell line, and primary cardiomyocytes are more relevant as they are closer to physiological conditions. Therefore, we will use primary cardiomyocytes for our further investigation to confirm our current findings. It should also be noted that there was no positive control in our experiments, which should be included in future studies.

Conclusion

In summary, we hereby report that Nerol alleviates H/R-induced injuries in H9c2 cells by promoting cell viability, attenuating apoptosis and oxidative stress via activating the PI3K/AKT signaling pathway. Therefore, our study suggests that Nerol could be used as a potential therapeutic strategy for H/R-induced injuries.

Conflict of interest

The authors declare that they have no conflicts of interest to disclose.

References

1. Essop MF. Cardiac metabolic adaptations in response to chronic hypoxia. *J Physiol*. 2007; 584:715-726.
2. Samaja M, Milano G. Editorial—Hypoxia and reoxygenation: from basic science to bedside. *Front Pediatr*. 2015; 3:86.
3. Morales CR, Pedrozo Z, Lavandero S, Hill JA. Oxidative stress and autophagy in cardiovascular homeostasis. *Antioxid Redox Signal*. 2014; 20:507-518.
4. Farías JG, Molina VM, Carrasco RA, Zepeda AB, Figueroa E, Letelier P, et al. Antioxidant therapeutic strategies for cardiovascular conditions associated with oxidative stress. *Nutrients* 2017; 9:966.
5. Zeng Y, Song JX, Shen XC. Herbal remedies supply a novel prospect for the treatment of atherosclerosis: A review of current mechanism studies. *Phytother Res*. 2012; 26:159-167.
6. Bagchi D, Sen CK, Ray SD, Das DK, Bagchi M, Preuss HG, et al. Molecular mechanisms of cardioprotection by a novel grape seed proanthocyanidin extract. *Mutat Res*. 2003; 523:87-97.
7. Guillermo Gormaz J, Quintremil S, Rodrigo R. Cardiovascular disease: a target for the pharmacological effects of quercetin. *Curr Top Med Chem*. 2015; 15:1735-1742.
8. Fathima SN, Murthy SV. Cardioprotective effects to chronic administration of Rosa Damascena petals in isoproterenol induced myocardial infarction: biochemical, histopathological and ultrastructural studies. *Biomed Pharmacol J*. 2019; 12:1155-1166.
9. Chen W, Viljoen AM. Geraniol — A review of a commercially important fragrance material. *South African Journal of Botany* 2010; 76:643-651.
10. Mileva M, Krumova E, Miteva-Staleva J, Kostadinova N, Dobрева A, Galabov AS. Chemical compounds, *in vitro* antioxidant and antifungal activities of some plant essential oils belonging to rosaceae family. *Comptes rendus de l'Académie bulgare des Sciences* 2014; 67.
11. Tiwari M, Kakkar P. Plant derived antioxidants—geraniol and camphene protect rat alveolar macrophages against t-BHP induced oxidative stress. *Toxicol In Vitro*. 2009; 23:295-301.
12. Menezes-Filho JERd, Souza Dsd, Santos-Miranda A, Cabral VM, Santos JNA, Cruz JdS, et al. Nerol attenuates ouabain-

- induced arrhythmias. *Evid Based Complement Alternat Med.* 2019; 2019:5935921..
13. Portal L, Martin V, Assaly R, d'Anglemont de Tassigny A, Michineau S, Berdeaux A, et al. A model of hypoxia-reoxygenation on isolated adult mouse cardiomyocytes: characterization, comparison with ischemia-reperfusion, and application to the cardioprotective effect of regular treadmill exercise. *J Cardiovasc Pharmacol Ther.* 2013; 18:367-375.
 14. Li C, Jackson RM. Reactive species mechanisms of cellular hypoxia-reoxygenation injury. *American Journal of Physiology-Cell Physiology* 2002; 282:C227-C241.
 15. Konstantinidis K, Whelan RS, Kitsis RN. Mechanisms of cell death in heart disease. *AAM J Physiol Cell Physiol.* 2012; 32:1552-1562.
 16. Kaufmann SH, Desnoyers S, Ottaviano Y, Davidson NE, Poirier GG. Specific proteolytic cleavage of poly (ADP-ribose) polymerase: an early marker of chemotherapy-induced apoptosis. *Cancer Res.* 1993; 53:3976-3985.
 17. Chaitanya GV, Alexander JS, Babu PP. PARP-1 cleavage fragments: signatures of cell-death proteases in neurodegeneration. *Cell Commun Signal.* 2010; 8:31.
 18. McIlwain DR, Berger T, Mak TW. Caspase functions in cell death and disease. *Cold Spring Harb Perspect Biol.* 2015; 7.
 19. Thomas RL, Roberts DJ, Kubli DA, Lee Y, Quinsay MN, Owens JB, et al. Loss of MCL-1 leads to impaired autophagy and rapid development of heart failure. *Genes Dev.* 2013; 27:1365-1377.
 20. Xu Y, Xing Y, Xu Y, Huang C, Bao H, Hong K, et al. Pim-2 protects H9c2 cardiomyocytes from hypoxia/reoxygenation-induced apoptosis via downregulation of Bim expression. *Environ Toxicol Pharmacol.* 2016; 48:94-102.
 21. Matsui T, Nagoshi T, Rosenzweig A. Akt and PI 3-kinase signaling in cardiomyocyte hypertrophy and survival. *Cell Cycle* 2003; 2:219-222.
 22. Duan W, Hicks J, Makara MA, Ilkayeva O, Abraham DM. TASK-1 and TASK-3 channels modulate pressure overload-induced cardiac remodeling and dysfunction. *Am J Physiol Heart Circ Physiol.* 2020; 318:H566-H580.
 23. Jiménez C, Hernández C, Pimentel B, Carrera AC. The p85 regulatory subunit controls sequential activation of phosphoinositide 3-kinase by Tyr kinases and Ras. *J Biol Chem.* 2002; 277:41556-41562.
 24. Matsui T, Tao J, del Monte F, Lee K-H, Li L, Picard M, et al. Akt activation preserves cardiac function and prevents injury after transient cardiac ischemia in vivo. *Circulation* 2001; 104:330-335.
 25. Yu JSL, Cui W. Proliferation, survival and metabolism: the role of PI3K/AKT/mTOR signalling in pluripotency and cell fate determination. *Development* 2016; 143:3050.
 26. Gobin B, Battaglia S, Lanel R, Chesneau J, Amiaud J, Rédini F, et al. NVP-BE2235, a dual PI3K/mTOR inhibitor, inhibits osteosarcoma cell proliferation and tumor development in vivo with an improved survival rate. *Cancer Lett.* 2014; 344:291-298.
 27. Durrant DE, Das A, Dyer S, Tavallai S, Dent P, Kukreja RC. Targeted inhibition of phosphoinositide 3-kinase/mammalian target of rapamycin sensitizes pancreatic cancer cells to doxorubicin without exacerbating cardiac toxicity. *Mol Pharmacol.* 2015; 88:512-523.
 28. Abraham DM, Lee TE, Watson LJ, Mao L, Chandok G, Wang H-G, et al. The two-pore domain potassium channel TREK-1 mediates cardiac fibrosis and diastolic dysfunction. *J Clin Invest.* 2018; 128:4843-4855.